ABSTRACT

CAO, WEI. Design of Temperature Sensors for Validation of Aseptic Food Processing. (Under the direction of Professor Paul D. Franzon).

With the increasing consumer demands for convenient, high quality, and healthy foods, aseptic processing was proposed as a potential option to meet these demands. In order to validate such a system and also make the process relatively inexpensive, researchers have to find out the "critical particle" in the processing system and determine its time-temperature history. The objective of this work is to develop and validate low power sensors that can be applied to monitor the internal temperature of particulates, as they flow through the heating, holding, and cooling sections of an aseptic processing system. The significance of this study lies in the development of a validated tool and technique that can be used to facilitate validating aseptic processing of multiphase foods and thereby provide the health-conscious consumer with a high quality food product.

Battery-powered off-the-shelf sensor had been successfully designed and tested. It was packaged in 1" plastic sphere, and the density was neutrally buoyant with water. It was able to work in the temperature range of 10°C to 150°C, with a potential accuracy of less than 1°C. The battery could last more than 20 hours. Integrated CMOS temperature sensors had also been investigated. The CMOS sensor design and simulation results are presented in details in this thesis. It had a total area of 0.054 mm^2, an averaged power consumption of 0.8 mW, and an accuracy of less than 0.2°C.

Design of Temperature Sensors for Validation of Aseptic Food Processing

by
Wei Cao

A thesis submitted to the Graduate Faculty of
North Carolina State University
In partial fulfillment of the
Requirements for the degree of
Master of Science

Electrical Engineering

Raleigh, North Carolina

2008

APPROVED BY:

_____	_____
Dr. Paul D. Franzon Committee Chair	Dr. Kevin Gard
_____	
Dr. K.P. Sandeep	

DEDICATION

To my parents, Chongzhi Cao and Guifen Zhang.

BIOGRAPHY

Wei Cao was born in Chengdu, Sichuan, China. He received the B.S. degree from Beijing Institute of Technology, Beijing, China, in 2001, majored in automatic control. He is currently a master student in electrical and computer engineering at North Carolina State University, Raleigh. His research focuses on analog/digital/mixed-signal circuit design. In fall of 2007, he was with Qimonda, working on 70nm DDR3 DRAM layout.

ACKNOWLEDGMENTS

I would like to express my sincere gratitude and thanks to my advisor, Dr. Paul Franzon, for his gracious support and continuous encouragement throughout my graduate study at the North Carolina State University. This thesis could not have been succeeded without his spirited guidance. I have learned innumerable lessons and insights from him on the workings of scientific research in general.

I also want to thank my committee members, Dr. K.P. Sandeep and Dr. Kevin Gard, for providing many valuable comments and suggestions that are essentially necessary for completion of this thesis.

Special acknowledgements are extended to Dr. Steve Lipa for his knowledgeable and valuable guidance, comments and suggestions to this work, and Mr. Harry Reinitz for the device packaging and testing. I would also like to thank all our research group colleagues for their valuable discussion, technical support, and other important contributions.

At last but not the least, I want to give my deepest gratitude to my parents, Chongzhi Cao and Guifen Zhang, for their endless love and moral support. This thesis is dedicated to them.

TABLE OF CONTENTS

LIST OF TABLES

LIST OF FIGURES

CHAPTER 1

Introduction

Food safety is rapidly becoming one of the most critically important issues in food industry. The quantitative measurement of the thermal process impact in terms of food safety and quality is essential in relation to the shelf life and acceptability (market and legal) of the product as well as for process optimization and control [1]. The objective of this project is to develop and validate low-power and high-performance sensors that can be applied to monitor the internal temperature of particulates, as they flow through the heating, holding, and cooling sections of an aseptic processing system.

1.1 Project Background and Motivation

With the increasing consumer demand for convenient, high quality, and healthy foods (and in accordance with CSREES goal #4 – "Improve the Nation's nutrition and health"), aseptic processing was proposed as a potential option to meet these demands. Although aseptic processing of liquid foods has been in place for several decades, how to process low-acid multiphase foods (foods containing large particles – for example, soups containing meatballs or vegetables) in an aseptic environment has still been an open question in U.S [2]. The main reason is that the FDA requires strict demonstration by conservative experimental validation

techniques and mathematical modeling of the process that every part of the food product receives adequate heat treatment to ensure commercial sterility [3].

In an attempt to address this problem, a workshop was organized by the Center for Advanced Processing and Packaging Studies (CAPPS) and the National Center for Food Safety and Technology (NCFST) in 1995 and 1996 [4]. The conclusions from the workshop were that determination of the residence time distribution (RTD) of at least 299 particulates in the product, determination of the heat transfer coefficient between the particulates and the fluid, and mathematical modeling are vital in process validation. To develop such kind of validation systems, the first and most important factor is the cost and time involved in the extensive process, which is partly due to the necessity to determine the RTD of 299 particles and the heat transfer coefficient between particles and the fluid [5]. This necessity arises due to the fact that we are currently unable to measure the time-temperature history at the "critical point" within particulates as they flow through the processing system [6]. Tetra Pak made use of the results from this study to successfully develop an aseptic process for a diced potato soup in a modified starch suspension and received a "no-objection" letter from the FDA for the process [7]. Although it demonstrated the feasibility of validating an aseptic process for multiphase foods, no such product was commercially marketed by any company in the U.S., majorly due to the high operational cost and long process time involved in this extensive validation, until Campbell Soup Co. went through a rigorous validation procedure to receive a no objection letter from FDA in 2006. Several food processors have been trying to develop a similar process for their food products and one of the main problems is the lack

of a reliable tool to validate their process and at the same time ensure a high product quality. The sensor system and validation protocol to be developed in this study will serve as that tool.

Generally speaking, “critical point” is the slowest heating portion of the product. For a food product containing only one type of particle, this is the center of the fastest moving particle. However, for a food product containing several types of particles, the “critical point” is the center of the slowest heating particle which may not necessarily be the fastest particle in the system. Thus, if we are able to determine the “critical particle” in a system and determine its time-temperature history, it would tremendously simplify the validation process and make the process relatively inexpensive.

Several methods have been attempted in the past to determine the internal temperatures of particles during continuous flow. However, all of these techniques were either “invasive” techniques that restricted the motion of the particles or non-invasive techniques that were not accurate. Thus, alternative approaches to “estimating” the internal temperatures of particles were devised. Some of the alternatives to measurement of the temperature at the “critical point” in a system have included biological techniques [8-10], moving thermocouple method [11-12], liquid crystal method [13-14], time-temperature integrators [1, 15-16], and melting point indicators [17]. Some of the techniques that could be used to measure the temperature within particles included the use of various forms of data trace (usually for retorting applications), thermochron iButtons (used for applications in large-scale systems),

paramagnetic implants within particles [18], ultrasonic tomography [19], micro-thermometry [20], change in proton precession frequency [21], magnetic resonance imaging [22], chemi-luminescent implants [23], thermo-magnetic switch implants [24], and fiber optic sensors [25]. However, all of these techniques are either expensive, elaborate, or difficult to incorporate in an aseptic processing system, or not accurate enough for process validation.

The significance of this study thus lies in the development of a validated tool and technique that can be used to facilitate validating aseptic processing of multiphase foods and thereby provide the health-conscious consumer with a high quality food product. It will pave the way for the development of new food products that were hitherto not developed due to the potentially low quality of the food (as a result of the inherent over-processing in the conventional retort process) in the absence of the tool to be developed in this study. Beyond that this sensor will also be useful in improving the quality of various thermal processes where accurate real-time temperature readings can minimize over-processing. It can also be used in some of the applications where time-temperature integrators are used to monitor the quality and safety of foods.

1.2 Thesis Overview

The thesis is organized into 6 chapters. Chapter 1, as an introduction, briefly describes the concept, motivation, and backgrounds of the development of temperature sensing techniques in aseptic food processing. The second chapter provides a detailed overview of this project. Existing temperature sensing techniques are reviewed and evaluated. Previous work and our

design flow, as well as the verification plan, are presented in this chapter. The design of the off-the-shelf temperature sensor is presented in detail in Chapter 3, followed by chapter four which contains the testing results and verification of the sensors. Chapter 4 also talks about the calibration, limitation, and possible future plan of the sensor. Chapter 5 discusses the basic CMOS temperature sensor design. It provides a technical overview on CMOS temperature sensing and on-board analog-digital conversion techniques. This chapter is then dedicated to the CMOS sensor design, including temperature sensor, internal clock, and a digital control ASIC. The results of the simulations using Cadence and Synopsis tool kit and the layouts of each part are presented. The last chapter, Chapter 6, is the conclusion and future direction for research.

CHAPTER 2

Project Overview

Temperature is one of the most widely measured phenomena in the process control environment. In this chapter, a detailed review of different types of existing temperature sensing techniques in aseptic food processing is presented, followed by a short discussion on temperature sensor calibration. The previous related development of temperature sensors in the Department of Food Science at NCSU is summarized in Section 2.3. The project objectives, design flow, as well as verification plan, are presented in Section 2.4.

2.1 Temperature Sensing Techniques Review

As in the food industry, the quantitative thermal measurement has a huge impact on the food safety and quality, as well as on the shelf life and acceptability of the products. If we are able to determine the critical particle in a system, which refers to the slowest heating portion of the product and thus usually but not always is the center of the fastest moving particle, and determine its time-temperature history, it would tremendously simplify the validation process and make the process relatively inexpensive. Various kinds of sensors are used in many fields in the industry and in household equipment, while here we are mainly focusing on those that have been applied to or have potentials in aseptic food processing. There are many

types of temperature sensors that use various technologies and have different characteristics [8-26]. Many common elements such as resistance temperature detectors (RTDs), thermistors, thermocouples or diodes, as well as some newly developed sensing methods using infrared, microwave, optical or biological techniques, have been used to measure absolute temperatures or temperature changes in various applications. It is maybe worth pointing out that noticeable difference exists between different temperature sensor or temperature measurement device types.

Food scientists and researchers have worked more than a decade attempting to determine the internal temperatures of food particles during continuous flow. The methods that they have used can be roughly classified into two groups: non-contact temperature sensors and contact sensors. The former are also called remote temperature sensors, and the latter could be further divided into two categories: external temperature sensors and internal temperature sensors. They are summarized in the Table 2.1, Table 2.2, and Table 2.3.

However, all of these techniques are either expensive, elaborate, or difficult to incorporate in an aseptic processing system. For instance, some of the "invasive" techniques are very sensitive but they tend to restrict the motion of the food particles. Meanwhile, those non-invasive techniques are just not able to provide accurate enough results for process validation. We are looking for a reliable yet accurate tool to validate their process and at the same time ensure a high product quality. The sensor system and validation protocol to be developed in this study will serve as that tool.

Table 2.1: Different remote temperature sensors.

Type	Working Principle	Comments
Temp sensor using external magnetic flux	Output resonant frequency changes with temperature	No power supply needed for sensor; accurate; relatively simple structure
Microwave temp sensor	Use X-band radiometer	Work in bad environment; more accurate than infrared sensors
Infrared temp sensor	Detect energy emitted by target	Only use 0.7-14 micron band
Optical fiber sensor		Work at high temperature; high resolution

Table 2.2: Different external (non-invasive) temperature sensors.

Type	Working Principle	Comments
Pt thermal sensor/heater		Easy to fabricate, calibrate and use; working as both heater and sensor
External sensor on the outer wall	Measure inside fluid temperature by converting the readings from external sensor	Able to calculate internal fluid temperature with external sensors, when insertion of a thermometer is impossible or impractical

Table 2.3: Different internal temperature sensors.

Type	Working Principle	Comments
CMOS/bipolar temp sensor		Extremely small and low power; will be discussed in chapter 4&5
Time-temperature integrator	Use enzyme system or peroxides immobilized on porous glass	
Melting point indicators	Color change	Able to measure the temperature inside of a particle
Liquid crystal temp sensor	Color change	Have to coat liquid crystal on monitored particle
Moving thermocouple		a classic, widely used method; motor-driven thermocouple moving along the tube
Temperature mapping (magnetic resonance imaging)	Precession frequency changes with temperature	

2.2 Temperature Sensor Calibration

One key secret to high quality temperature measurement results is to have a careful calibration before any tests. Without reliable calibration, the results will always be questionable and hardly worth the effort and cost. Uncertainties result from various factors, including: sensor tolerances, which are usually specified according to published standards and manufacturers specifications; instrumentation (measurement) inaccuracies, again specified in manufacturers specifications; drift in the characteristics of the sensor due to temperature cycling and ageing; possible thermal effects resulting from the installation, for example thermal voltages created at interconnection junctions. A combination of such factors will constitute overall system uncertainty [26].

Temperature sensor calibration provides a means of quantifying uncertainties in temperature measurement in order to optimize sensor and/or system accuracies. It is achieved by elevating the temperature sensor to a known, controlled temperature and measuring the corresponding change in its associated electrical parameter (voltage or resistance). If the sensor is connected to a measuring instrument, the sensor and instrument combination can be effectively calibrated by this technique [27].

In order to achieve high accuracy, piecewise linearization method is widely used in the calibration process. It is done by repeating the calibration process described in last paragraph

at multiple temperature points. Then plug in the recorded data to the function below and determine values for A and B.

$$T = A1*V + B1 \tag{1}$$

where T is the known temperature, V is the recorded voltage output of the temperature sensor, A and B are constants to be determined.

As a result, we can get the following equation:

$$\begin{cases} T = A1*V + B1 & \text{where } 0.2 > V \geq 0; \\ T = A2*V + B2 & \text{where } 0.4 > V \geq 0.2; \\ T = A3*V + B3 & \text{where } 0.6 > V \geq 0.4; \\ T = A4*V + B4 & \text{where } V \geq 0.6; \end{cases} \tag{2}$$

where T is the temperature we want to get, V is the recorded voltage output of the temperature sensor, A1-A4 and B1-B4 are known constants.

Table 2.4 shows the inaccuracy of available temperature sensors in our lab.

Table 2.4: Inaccuracy of available temperature sensors in lab.

Name	Inaccuracy	Comments
LM94021 temp sensor	+/- 2.71 °C	
Handheld digital thermometer	+/- 0.89 °C	Easy to use; hard to keep a long-time record
Data acquisition unit	+/- 1.25 °C	Very flexible; provide digital output of temperature history

So as a starting point, we should use either the handheld digital thermometer or the data acquisition unit to calibrate the temperature sensors. To further increase the sensor accuracy,

we might adopt a secondary standards system for high quality comparison and fixed point measurements which would provide accuracies generally between 0.1°C and 0.01°C.

2.3 Previous Work on Temperature Sensing in Department of Food Science

Several sensors have been developed in the Department of Food Science at NCSU in the past few years that can be used to determine the time-temperature history within simulated, conservatively constructed implant-carrier particles.

In those sensors, both implants and carrier particles were designed and implemented to be robust and inexpensive so that the tagged particles can be disposed after a single use in order to satisfy the limitation requirements on their re-use. Throughout all these work they have thus established a theoretical and practical basis for the design, construction, and validation of conservative properties of implant carrier particles. Such method and approach could serve to reduce the number of particles that need to be monitored and recorded. Software has been developed to "design" a particle that would exhibit conservative thermal and flow behavior. The main goal here is to construct a "conservative" particle that would receive less thermal treatment than any other particle in the system and for us to monitor the time-temperature history within this particle. As long as this "conservative" particle receives sufficient heat treatment, the entire product would receive adequate heat treatment and hence the product would be rendered commercially sterile. Previous studies have shown that near neutrally buoyant particles are the ones that travel fastest through a system and thus receive the least

thermal treatment. Therefore, we have to ensure that the entire particle of our temperature sensor is nearly neutrally buoyant with water and thus exhibits conservative flow behavior.

2.4 Project Overview

The current study will be undertaken with the goal of providing a reliable and quick way to determine the temperature at the "critical point" within an aseptic processing system to facilitate process validation. The technique will involve the development of sensors that can be used to determine the internal temperature of food particles as they flow through the heating, holding, and cooling sections of an aseptic processing system. The sensor will then be implanted in the cavity of a "conservatively" designed carrier particle such that the thermal treatment delivered to the center of this particle will always be less than that received by every other particle in the real food product.

2.4.1 Project Requirements

Listed below are the specific requirements and/or preferences of the temperature sensors in this project:

a. Low power consumption (a very critical issue due to battery duration requirement; ideally in the order of 1mW or less);
b. Small volume (ideally 8mm x 8mm x 8mm or less; must fits in the target package), which can also be interpreted as a low need of gates if we use CMOS sensor;
c. Density of around 1 g/cm^3 (therefore it would be neutrally buoyant with

water);

d. Easy calibration (which means it only needs one or two point calibration; curvature correction to be used only if necessary);
e. Favorably digital output signal (easy to interface with built-in memory chip as well as RF circuit);
f. A temperature range of 25-125 (or 0-150) °C;
g. Inaccuracy of 1 °C or less;
h. Low cost and/or good reusability, which could greatly reduce the running cost of such a validation system;
i. Easy to program, integrate, interface, and package if we use commercially available sensor chip; or
j. Compatible with target process without additional expensive fabrication steps, if we build custom CMOS thermal sensor (here, it means it has to be compatible with the rest of the circuit such as the RF part)

2.4.2 Design Flow

This work has been divided into two main stages, which involves with the development of off-the-shelf sensor and CMOS sensor respectively. In the first stage, off-the-shelf sensor is built up using commercially available components. The system consists of a low-power microcontroller with analog-digital converter, a temperature sensor chip, a FLASH memory chip for logging data, and a high-temperature coin battery to supply power. All components will have to be qualified for working at 125-150 °C. In particular, the battery should be able

to provide at least 30 minutes of adequate power supply to the unit, while handling both the high temperature and the pressure encountered in aseptic processing.

Development of the off-the-shelf sensor will proceed in three steps. In the first step, candidate components will be combined using normal printed circuit board techniques to verify proper operation of the system and to allow for optimization of performance. Please refer to the next section for a detailed verification plan. This step will provide us with experience of programming and interfacing between different chips. After the final selection of components is made, the second step will commence, during which the sensor will be shrunk to the dimensions necessary for insertion into the carrier particle. The goal is to obtain the smallest feasible particle size while matching the density of the food being processed. When the design is finalized, we will pursue the last step, where we do a low-level manufacturing to produce a collection of these sensors (quantity based on requests from individual companies and consortiums such as the Center for Advanced Processing and Packaging Studies -- CAPPS) for use by food processors in validating a multiphase aseptic process.

After that, integrated CMOS temperature sensor will be investigated. Thanks to the advanced IC processing technology, CMOS sensors are able to provide low-cost and high-performance solutions in the area of temperature sensing. Compared to off-the-shelf temperature sensors, the CMOS sensors have the advantages of smaller area and lower power consumption.

The CMOS temperature sensor includes an analog temperature sensor, a current to frequency converter, an internal clock, and a digital control unit. The output signal of the current to frequency converter is a square-wave which carries the temperature information from the sensor. This frequency is then turned into a digital number by counting the square-wave pulses in the digital control unit, and it stores the information in the flash memory. The design and simulation results will be presented in Chapter 5, followed by a short discussion about RFID and RF telemetry.

2.4.3 Validation Plan

The verification includes two phases. The first phase in developing sensors of this kind will involve testing of the module developed to ensure that it performs as per the requirements of the application. This step includes, but not limited to, the testing of A/D conversion, proper flash memory I/O, device performance at high temperature and the duration of battery.

The second phase of the validation studies will involve determination of the accuracy of measurement of temperature. This will be divided further into two parts -- batch test (zero relative velocity between the fluid and particle) and continuous flow test (maximum relative velocity between particle and fluid). Thus, the validation of the sensor system for the widest possible range of parameters (from a relative velocity and hence heat transfer coefficient standpoint) would ensure that the sensor system would conservatively determine the temperature within the particle at any intermediate processing condition. Batch tests are conducted with thermocouples inserted at the center of the packaged temperature sensor. The

particles are heated in an autoclave, and temperature data from the thermocouple is gathered using a data acquisition system. By comparing the reading from our temperature sensor and the reading from the data acquisition system, we can determine the accuracy of our sensor. A calibration will also be done in this step to improve the accuracy. In the continuous flow test, a particle will be immobilized in the flow regime so as to achieve the maximum possible relative velocity between the particle and the fluid. The temperature at the center of the simulated particle that contains the sensor will also be measured using a thermocouple. The sensor will be re-tested and modified in case it yields a temperature reading higher than that of the thermocouple.

CHAPTER 3

Off-the-shelf Sensor Design

As the first stage of this project, off-the-shelf sensor was built up using commercially available thermometer chip, microcontroller, and memory chip, to evaluate the effectiveness of each component for this application. The evaluation included but not limited to the measurement precision, high temperature working performance and duration of the battery.

The sensor was required to operate at temperatures much higher than the normal commercial temperature range (0-70°C) of electronic components. All components had to be qualified for operation at 125-150°C. As the innermost part of the probe, it was not subjected to the highest temperatures in the system during normal operation, but it still had to withstand sterilization temperatures while not in operation. These considerations limited the selection of components for use in the sensor, but fortunately there were components available that could do the job. The main issues in the design of the sensor included the volume budget, component availability, performance of components that operate at extreme temperatures, sensor accuracy, memory capacity for data logging, and battery capacity.

In this chapter, we first discuss the selection of each component. Major design considerations, as well as some preliminary testing results, are included in this chapter, which serves to justify our hardware and/or software design. Then the hardware design is presented, followed by a brief software development overview. The last part is a brief conclusion of the off-the-shelf sensor design.

3.1 Component Selection

3.1.1 Microcontroller

The brain of the data logging system is a microcontroller. Microcontrollers are highly integrated microprocessors designed specifically for use in embedded systems. They typically include an integrated CPU, memory (a small amount of RAM, ROM, or both), and other peripherals on the same chip. Table 3.1 is a partial list of the potential microcontroller candidates that we considered. Three main factors in determining the best choice was their size, power consumption and temperature range. From Table 3.1, we could see that Texas Instrument MSP430F2012 offers the best combination of those three. There are lots of nice features about this microcontroller which will be discussed and utilized later in this thesis.

3.1.2 Battery

The selection of a battery was complicated due to the requirement that it should be able to withstand temperatures above 125°C and handle the pressures encountered in aseptic processing. A number of companies offered batteries that worked at very high temperature, but most high-temperature applications did not require miniaturization and some of these

battery chemistries did not scale to small sizes well. Five possible candidates are shown in Table 3.2.

Table 3.1: List of potential candidate microcontrollers with specification.

	Size (mm) L x W x H	Temperature Range (°C)	A/D Bit	Input #	Operation Current	Standby Current
TI MSP430F2012	5.1 x 6.2 x 1.2 (14 PSOP)	-40 to 105	10	5	< 220 µA	0.5 µA
TI MSP430F1122	5.2 x 5.2 x 1 (QF) 3 x 6 x 1.2	-40 to 85	10	5	< 200 µA	0.7 µA
Microchip PIC10F	2.8 x 2.95 x 1.18 (6 Pin)	Extended to -40 to 125	8	2	<170 µA	100 µA
Atmel AT91SAM7S321	7 x 7 x 0.9	-40 to 85	10	8	<10 mA	60 µA
National Semi COP8SBR9	7 x 7 x 0.8 (QF) 12 x 8 x 1.1	-40 to 125	10	6	130 µA	30 µA
Dallas Semi MAXQ3120	24 x 18 x 1	-40 to 85	16	2	~3 mA	250 µA
ST Microelect ST6200C	6 x 8 x 2	-40 to 125	8	4	~2 mA	~100 µA
ST Microelect ST7LITEUS2	4.5 x 3.5 x 0.9 (QF)	-40 to 85	10	5	~2 mA	~100 µA
Philips P89LPC9102	3 x 3 x 1 (QF) 5 x 6.5 x 1	-40 to 85	8	4	~3 mA	~1 mA

Table 3.2: List of potential candidate batteries with specification.

	Panasonic BR-1225A	Cymbet CPF080809L	ABLE ER10240S	Sony SR512	Tadiran TLH2450
Capacity	48 mAh	200 µAh	320 mAh	6 mAh	550 mAh
Voltage	3 V	3.8 V	3.6 V	3V	3.6 V
Temp Max	125°C	70°C	150°C	60°C	125°C
Diameter	12.5 mm	8 mm	10 mm	5.8 mm	24 mm
Height	2.5 mm	0.9 mm	12 mm	1.25 mm	6 mm
Weight	0.8 g	0.4 g	6 g	0.13 g	10.8 g

The size and temperature requirements left us to the only choice of Panasonic BR-1225A. It was a 3V, lithium coin shaped battery that weighs only 0.8 g and provides 48 mAh at 125 °C.

Assuming that the sensor would be in operation for approximately 20 minutes at a time the Panasonic battery could allow approximately 100 uses before requiring replacement.

Thin film battery was another possibility, and it had some other good features such as rechargeability and flexible overall size. However, for the time being, available thin film batteries were too large to be used in our project, although some vendors could do custom sizes if the business opportunity warranted, and there might be something close to our requirements in next a few years.

3.1.3 Temperature Sensor

We had been looking for commercially available temperature measurement ICs for a couple of months. The requirements and preferences of these ICs have been explicitly stated in Chapter 1. There were several temperature ICs we had found that were capable of measuring temperature above 125°C. Several possible candidates are shown in Table 3.3.

Since it was desirable to have temperature go to 150°C, we finally chose the analog temperature sensor LM94021 by National Semiconductor. It had a wide temperature range, very small layout, extremely low power consumption, and selectable gains. Only shortcoming was its accuracy was not the best, which we hoped could be compensated by a good calibration and post-experiment data processing.

Table 3.3: List of potential temperature sensors with specification.

	Temp Range (°C)	Output Type	Supply Current	Accuracy (°C)	Size (mm)	Other Comments
TI TMP106	-40 to 125	9 or 12 Digital	50 μA	+/-3.0 (max)	1 x 1.5 x 1.6 (BGA)	2-wire serial interface
National LM74	-55 to 150	12 Digital	~ 300 μA	+/-3.0 (max)	5 x 6 x 1.3	*
National LM94021	-50 to 150	Analog (V)	9 μA	+/-2.7 (max)	2 x 1.8 x 1	Off mode; Selectable Gains
Dallas Semi MAX6641	-40 to 125	8 Digital	~ 500 μA	+/-1	3 x 5 x 1.1	2-wire serial interface
Dallas Semi MAX1464	-40 to 125	16 Digital	~ 2 mA	+/-2	6 x 7.6 x 1.7	Signal conditioner
Fairchild FM20	-55 to 130	Analog	< 30 μA	+/-2.5°C	2 x 2 x 1	Cheap, Ultra low power
National LM20BIM7	-55 to 130	Analog	~ 50 μA	+/-5°C (max)	2 x 1.8 x 1	Low power, accurate, *

*: which also comes with ball grid array package with a much smaller size

3.1.4 Memory Chip

Memory chip was used to store data obtained by thermal sensor. They were preferred to have small chip size, low power dissipation and proper working temperature range. SRAMs and Flash memory chips are listed separately in Table 3.4 and Table 3.5, respectively. Some chips were too large to be fitted in the targeted package, such as SRAM AS8SLC512K32 from Austin Semiconductors or SRAM μPD448012-X from NEC, so that they are not even listed in the tables.

The size of the memory should large enough to store the data of monitoring temperature as a function of time for periods of up to 30 minutes, assuming a maximum sampling rate of 100 times per second. Therefore, at least several megabits were needed in this project.

Since flash memory had the advantage of maintaining data when power goes off, it was preferred in our project. Our final choice was Atmel flash memory AT45DB041B, which had a small layout yet enough memory space to store all the data. It had a wide working temperature range of -55 to 125°C, which was the best situation we had ever met. Its serial peripheral interface also made the microcontroller programming easier and more efficient.

Table 3.4: List of potential SRAM memory chips with specification.

	Cypress CY62167DV30	Nanoamp N16T1630C2B	Hynix HY64SD16162B
Memory Size	16 MB	16 MB	16 MB
Memory Type	SRAM	SRAM	SRAM
Active Current	2 mA	2 mA	20 mA
Standby Current	2 µA	100 µA	10 µA
Temp Range	-65 to 125°C	-40 to 85°C	-40 to 85°C
Area (mm)	8 x 9.5 x 1 (BGA)	6 x 8 x 0.9 (BGA)	6 x 8 x 1 (BGA)

Table 3.5: List of potential FLASH memory chips with specification.

	Atmel AT45DB041B	STMicroelectronics M29W160	Sharp LH28F160S3HN	Intel 28F016/160B3
Memory Size	4 MB	16 MB	16 MB	16 (or 8, 32)MB
Memory Type	Flash	Flash	Flash	Flash
Active Current	4 mA	20 mA	15 mA	10 mA
Standby Current	2 µA	100 µA	2 µA	10 µA
Temp Range	-55 to 125°C	-40 to 85°C	-40 to 85°C	-40 to 85°C
Area (mm)	5.2 x 8 x 1.4	6 x 8 x 1.2 (BGA)	12 x 20 x 1.1	7 x 7.3 x 1 (BGA)

A complete list of all the components is shown in Table 3.6.

Table 3.6: Complete component list.

	MPU	Flash Memory	Temp Sensor	Battery
Part Name	TI MSP430F2012	Atmel AT45DB041B	National Semi LM94021	Panasonic BR-1225A
Temp Range	105°C	125°C	150°C	125°C
Size (mm)	5.1 x 6.6 x 1.2	5.2 x 8.0 x 1.2	2.0 x 2.0 x 1.0	12.5(D) x 5.5
Comments	10-bit ADC	4MB Storage	X-Low Power	0.8 gram

3.2 Design Considerations

Before we talk about the hardware and software design, we need to review some of our design considerations, as well as some preliminary testing results, which led us to our final hardware and/or software design.

3.2.1 Clock Source

The MSP430 platform of ultra-low-power 16-bit RISC mixed-signal processors from TI provided the ultimate solution for battery-powered measurement applications [28]. Its clock system was designed specifically for battery-powered applications. A low-frequency auxiliary clock (ACLK) was the default clock when driven directly from a common external 32-kHz watch crystal.

If the ACLK was not available, an integrated high-speed digitally controlled oscillator (DCO) could then source the master clock (MCLK) used by the CPU and high-speed peripherals. The DCO frequency could be adjusted, from 60 kHz to 24 MHz, by software using the DCOx, MODx, and RSELx bits, which is shown in Figure 3.1.

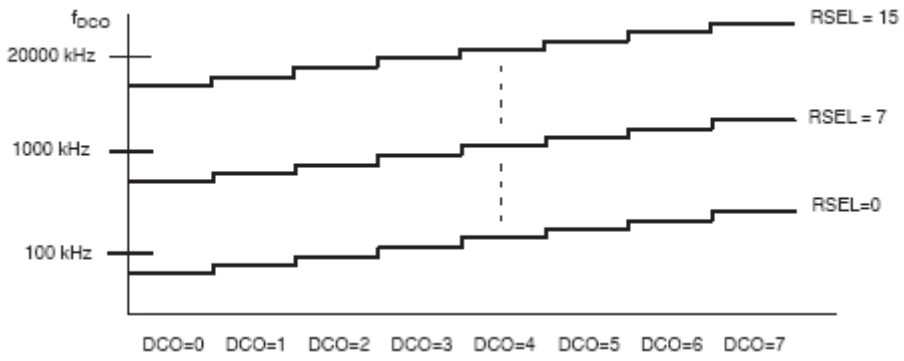

Figure 3.1: Typical DCOx range and RSELx steps vs. f_{DCO}.

The ACLK had two main advantages over the DCO. It was very stable with ambient temperature change, and it enabled the low power mode of MSP430F2012 because we could then disable the DCO. However, the testing results showed that the 32 kHz was not high enough to execute a sample rate of 1 per second. In order to make sure our sensor system have the flexibility to change the sampling rate up to 100 per second, we chose to use the internal DCO as our primary clock source.

Figure 3.2 shows the MSP430F1xx series microcontroller DCO frequency relationship with temperature. There was a 25% frequency swing over temperature range (25 to 100°C). In the user's guide of MSP430F2xx series microcontroller, it stated that the DCO temperature stability had been significantly improved since MSP430F1xx series. There was no figure about the DCO frequency relationship with temperature. Therefore we assumed that the DCO in our microcontroller was stable with different temperatures. And our testing results confirmed our assumption that there was no noticeable frequency variation over the

temperature range of 0 to 150°C. In case the frequency variation need to be further reduced, it could be software-corrected since it had an almost linear relationship with temperature change.

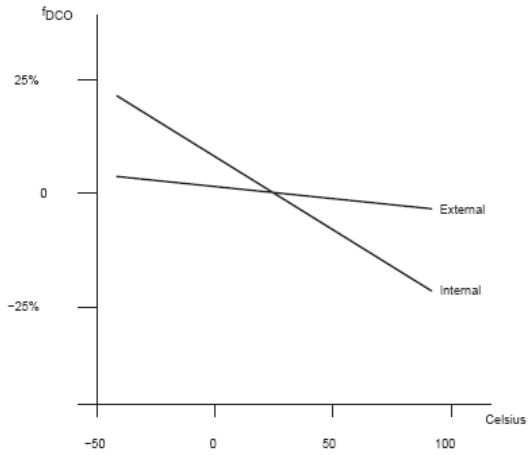

Figure 3.2: DCO frequency vs. temperature.

3.2.2 Sampling Rate

According to the requirement of our colleagues from food science department, the sampling rate would be between 1 to 100 samples per second. The higher the sampling rate was, the higher the DCO frequency must be. Figure 3.3 shows the relationship between active current and $f_{DCO.}$ To achieve 100 samples per second, the DCO frequency had to be set above 16 MHz. The required current was beyond the capacity of the BR1225A battery, which led to failure in flash memory writing.

Our testing results showed that the sampling rate of 50 samples per second was feasible. In this case, f_{DCO} was around 10 MHz, and the battery could last more than 4 hours. In order to

save battery power, we used a sampling rate of 5 samples per second in most of our tests, where f_{DCO} was around 0.8 MHz, and the battery lasted more than 16 hours.

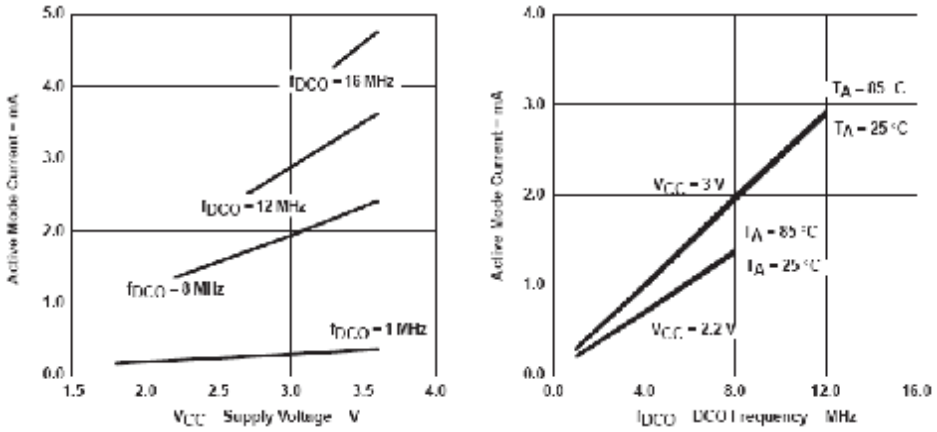

Figure 3.3: Active mode current vs. VCC, TA, and f_{DCO}.

3.2.3 Battery Capacity and Voltage

Table 3.7 shows the specification of our battery BR1225A [29]. Note that although the nominal voltage is 3V, but at room temperature it drops below 2.7V, as shown in Figure 3.4, which is below the threshold of flash memory chip. In our test, it was about 2.3V when battery was hooked up to the device at room temperature. As a result, we had to stack two of these batteries together to power our device to make sure of the proper behavior of the temperature sensor over its designed working range. This issue will be further discussed in next chapter, with more detailed testing results and possible alternative solution.

Table 3.7: BR1225A specification.

Diameter	Depth	Weight	Nominal Voltage	Nominal Capacity	Continuous load	Operation Temperature
12.5 mm	2.5 mm	0.8 g	3 V	48 mAh	0.03 mA	-30 – 125 °C

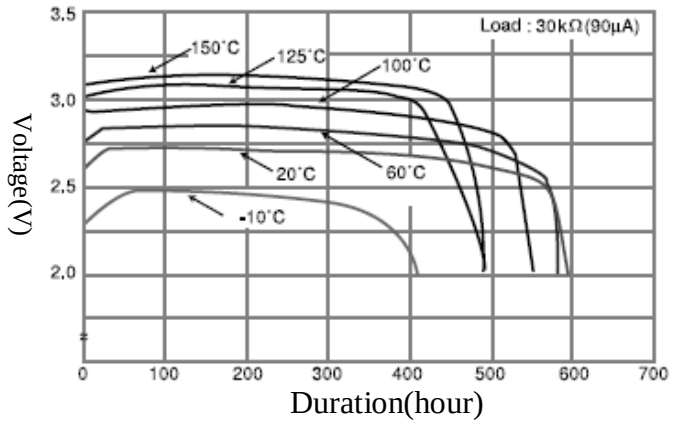

Figure 3.4: BR1225A temperature characteristics.

3.2.4 Serial On-Board Programming

One nice feature that MSP430 series microcontrollers provided was the serial on-board programming. With the proper connections, the C-SPY debugger and an FET hardware JTAG interface, such as the MSP-FET430UIF used in our project, could be used to program and debug code on a target board. By doing this, it provided us with an easy way to re-program microcontroller, if any changes were necessary. It also was a good interface when we wanted to read the data from flash memory after any tests.

Figure 3.5 shows the connections between the 14-pin FET Interface module connector and the target device required to support in-system programming and debugging using C-SPY for 2-wire Spy-Bi-Wire communication.

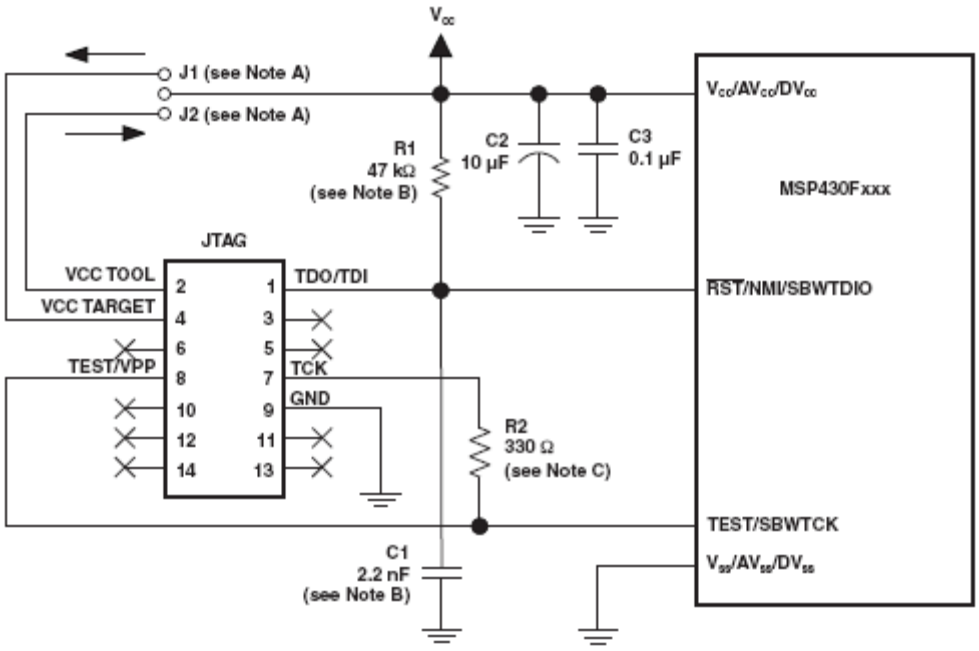

Figure 3.5: Signal connections for 2-wire spy-bi-wire communication.

3.2.5 File I/O

After any tests, there would be lots of data we have to get out from flash memory. At first we had to look into the memory, through the microcontroller, bit by bit to get those numbers. Obviously it was time-consuming and very prone to errors. So we thought it would be a good idea to have file I/O function in our software that all the numbers were outputted into a text file automatically. However, the normal file I/O functions, i.e. fopen and fprintf, did not work with the microcontroller due to the limit of heap size. Therefore an alternative plan was derived where we used a virtual terminal I/O to output the numbers that we want. Also due to the limit of heap size, the microcontroller could not handle floating number. So we had to use another regular C program to convert the decimal data into temperature.

3.2.6 Power Saving Techniques

Low power operation is a key point in this project. If we can dramatically reduce the whole power consumption, there are lots of benefits we can get. The same battery could be used for a longer time, or smaller batteries could be adopted, or the operation frequency could be increased without draining extra battery power. Low power mode (LPM) is a key feature of the MSP430 serial microcontrollers. Its design gives very low leakage, and it operates from a single supply rail. This gives an extremely low current drain when the processor is in standby mode. It could be waked up by an interrupt event such as Timer_A, which was used in our application.

Listed below are the major techniques that we had adopted in our sensor design:

a. Set the microcontroller frequency at the lowest possible level while the sampling rate can be met;
b. Let the microcontroller enter low power mode while doing analog to digital conversion;
c. Let the microcontroller enter low power mode while waiting for flash memory writing process (microcontroller being waked up by Timer_A);
d. Turn temperature sensor into standby mode when possible;
e. All unused pins are left open, switched to I/O port function, and configured as outputs, to prevent any unnecessary power consumption; and
f. Let the microcontroller enter low power mode while waiting for device

packaging and experiment setup (in this case, the power saving is not only from microcontroller, but, more importantly, from letting the flash memory into standby mode).

3.3 Sensor Design - Hardware

3.3.1 System Schematic and PCB Design

A system schematic of our off-the-shelf temperature sensor is shown in Figure 3.6. Two BR1225A batteries were used as power source in the sensor system. A decoupling capacitor was necessary in this project. Without that, the current provided by batteries themselves was not enough when data were written to the flash memory. The microcontroller converted the analog voltage signals from the temperature sensor into digital numbers. After that, data were stored in the Atmel flash memory in binary format. A two-sided printed circuit board (PCB) was designed with EAGLE. The layout was shown in Figure 3.7. The size of the board was smaller than 10 mm by 9 mm. If we use surface-mount decoupling cap and power switch, the overall dimension can be shrunk down to 8 mm by 7 mm.

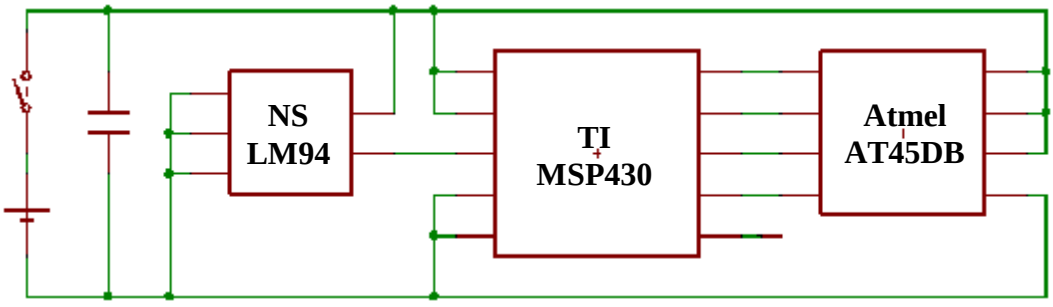

Figure 3.6: System schematic of our temperature sensor.

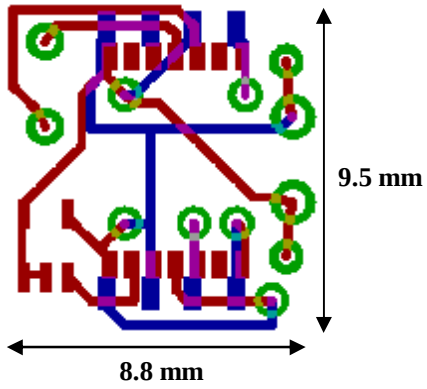

Figure 3.7: PCB layout of our temperature sensor.

Our off-the-shelf temperature sensor is shown in Figure 3.8. The overall dimension was 12.5 x 12.5 x 9 (mm) with two batteries, or 12 x 12 x 4 (mm) without any battery.

Figure 3.8: Off-the-shelf temperature sensor (left top: front view w/o battery; left bottom: front view with batteries; right top: back view; right bottom: horizontal view with two batteries).

3.3.2 On-Board Programming Setup

The on-board programming setup is shown in Figure 3.9. On the left side of the picture was the MSP-FET430UIF which connected the setup to the USB port on a desktop PC. This setup was used for debugging, re-programming, and data reading.

Figure 3.9: On-board programming setup.

3.4 Sensor Design - Software

3.4.1 Microcontroller Programming - Write

Microcontroller had been successfully programmed in C using IAR Embedded Workbench, which is a very powerful Integrated Development Environment, which allows users to develop and manage complete embedded application projects.

Before we start to talk about the code, we should first review the working principles of the flash memory used in our project. The AT45DB041B is a serial interface Flash memory. Its 4,325,376 bits of memory are organized as 2048 pages of 264 bytes each. In addition to the main memory, the AT45DB041B also contains two SRAM data buffers of 264 bytes each.

By specifying the appropriate opcode and then following the required steps, users can either write data to it or read data from it. To initiate a write operation, an 8-bit opcode of 82H must be followed by the four reserved bits and 20 address bits. After all address bits were shifted in, the part took data from the SI pin and stored it in one of the data buffers. When there was a low-to-high transition on the CS pin, the data stored in the buffer was transferred into the specified page in the main memory. Following is the pseudo code:

```
void main(void) {
  Stop Watch-Dog Timer(WDT);
  Setup DCO frequency;
  Enable and setup 10-bit ADC;
  Packaging_standby ();
  Setup I/O directions;

  for (Page = 0; Page < 2048; Page ++)  {
     for (Byte = 0; Byte < 264; Byte = Byte + 2)  {
          Start ADC;
          Shift in opcode (82H) and 20 address bits;
          Store 10-bit ADC result in flash memory;
          All inputs finished, set CS to be high;
          Data_transfer_standby(); } }
}
```

3.4.2 Microcontroller Programming - Read

After the test, we had to pull data out from the flash memory, so another program was designed to do this job. To start a read operation, an opcode of 52H must be clocked into the flash memory chip, followed by 24 address bits and 32 don't care bits. After that, additional pulses on SCK resulted in serial data being output on the SO (serial output) pin. A low-to-high transition on the CS pin terminated the read operation and tri-state the SO pin. All data was saved in a text file named "TermIO.log". It took a few hours to output all data from memory chip. Following is the pseudo code:

```
void main(void) {
  Stop Watch-Dog Timer(WDT);
  Setup Max DCO frequency;
  Setup I/O directions;

  for (Page = 0; Page < 2048; Page ++)  {
     for (Byte = 0; Byte < 264; Byte = Byte + 2)  {
          Shift in opcode (52H), 20 address bits, and 32 don't care bits;
          Read the 10-bit ADC result stored in flash memory;
          Convert binary number to decimal;
          Printf();
          All inputs finished, set CS to be high; } }
}
```

3.4.2 C Programming - Conversion

After we got the file “TermIO.log”, we used another regular C code to convert decimal numbers into real temperatures. The results were saved in a text file named “temperature_log.txt”. Following is the pseudo code:

```
void main(void) {
  char record[100], *fld;
  FILE * fin;
  FILE * pFile;
  fin = fopen("TermIO.log", "r");
  pFile = fopen ("temperature_log.txt","w");

  while (fgets(record, sizeof(record), fin) != NULL)  {
     fld = strtok(record, " \n\0\r\t");
     Decimal = atoi(fld);
     Voltage = decimal2voltage (Decimal);
     Temperature = voltage2temperature (Voltage);
     fprintf (pFile,"%f ",Temperature);
     fprintf (pFile,"\n"); }

  fclose(fin);
  fclose (pFile); }
```

CHAPTER 4

Off-the-shelf Sensor Testing and Verification

Off-the-shelf temperature sensor was successfully developed as described in last chapter. In this chapter, we mainly focus on the sensor testing and verification. After device packaging and the experiment setup is introduced, we show some primary measurement results in validation phase I in section 4.2. In section 4.3, we present the validation study phase II which determines the accuracy of temperature measurement. At the end of this chapter are the discussion and proposal for future work.

4.1 Device Packaging and Experiment Setup

The off-the-shelf sensor must be carefully and properly connected and packaged for it to collect temperature data from a test environment. In short, a ¾" polypropylene sphere was cut in half, as shown in Figure 4.1. Then the sensor was loaded in it, and sealed by aluminum tape, as shown in Figure 4.2. The experiment setup is shown in Figure 4.3. The black unit next to the desktop PC was the data acquisition device with Omega thermocouples. The black oven in the back was an autoclave used to heat up the sensor for the batch validation studies.

Figure 4.1: Prepare the polypropylene hemispheres.

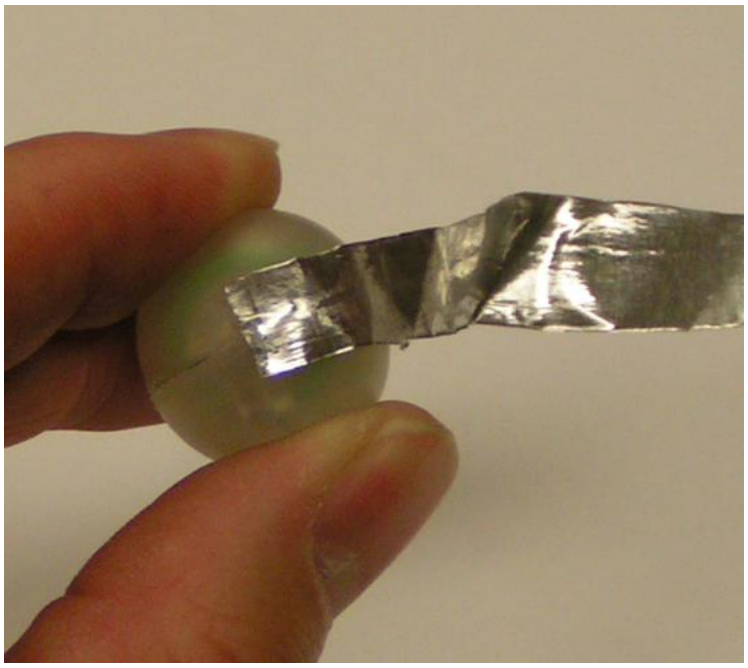

Figure 4.2: Sensor packaged in ¾”spheres.

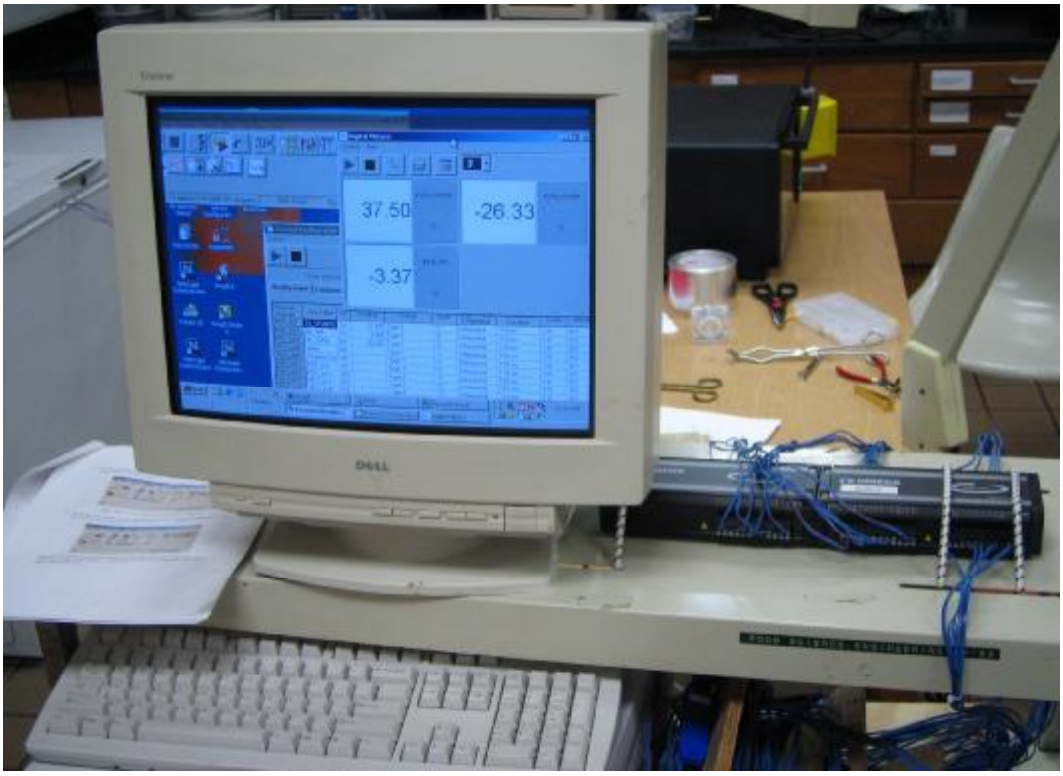

Figure 4.3: Experiment setup for the batch validation studies.

4.2 Validation Phase I

4.2.1 Physical Measurements

The sensor particle had to be neutrally buoyant with water so that it would not sink during the aseptic processing. Therefore, physical parameters were first measured in order to calculate the density of the particle. We found out that, although the sensor could fit in the ¾" sphere package, the density (1.21 g/cm^3) was much higher than water (~ 0.95 g/cm^3 @100°C). Thus we changed to 1" sphere and repeated the calculation. Results are shown in Table 4.1. This time the density was lower than water, which meant that we could add weight

to make it work. For example, to obtain neutral buoyancy at 100°C, approximately 2 gram should be added inside the sphere. Magnets or small RFID tags could be added for the purpose of position tracing. A sensor in 1" sphere package is shown in Figure 4.4. There was still lot of space left. The yellow item next to the sensor was a piece of magnet used to balance the weight.

Table 4.1: Density calculation of off-the-shelf sensor packages.

	Size (mm)	Volume (cm^3)	Weight (g)	Density (g/cm^3)
Sensor before Packaging	12.5 x 12.5 x 9	-	2.93 g	-
Sensor in ¾" Sphere	-	3.619	4.47 g	1.21
Sensor in 1" Sphere	-	8.58	6.15 g	0.716

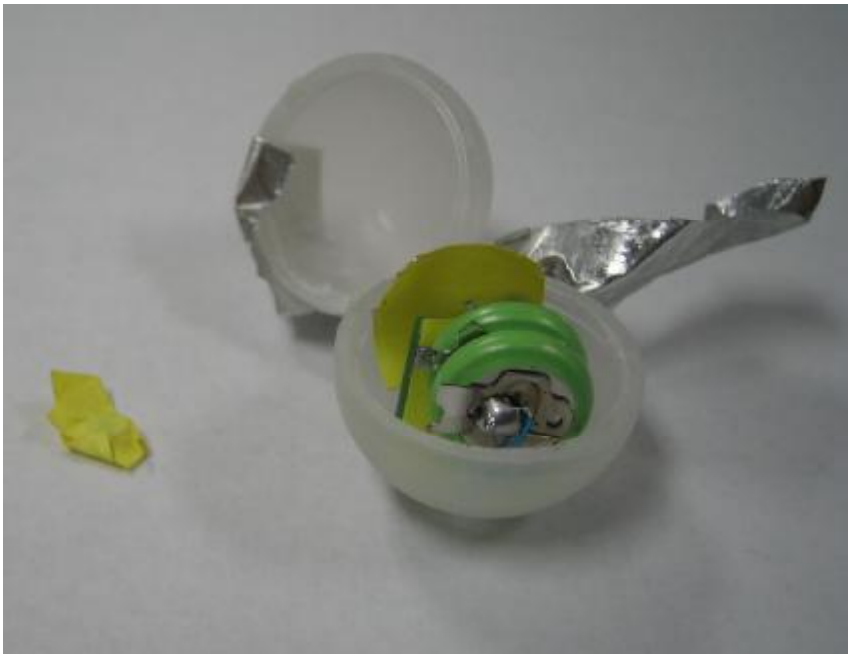

Figure 4.4: A sensor packaged in 1" sphere.

4.2.3 Battery Duration

Battery duration was also measured in tests. Results showed that at high sampling rate (50 samples per second) the two batteries could last more than 4 hours. At normal sampling rate (5 samples per second) the batteries lasted more than 16 hours. Beyond that time, microcontroller and temperature sensor were still working properly, but error began to occur in flash memory writing.

4.2.4 Temperature Measurement Range

Range of temperature measurement was roughly determined to be 10-140°C. The highest temperature our sensors had ever recorded was about 140°C. Although we had not tried 150°C, majorly due to lab safety concerns, we believe there are good chances that this sensor could work at 150°C.

The sensor failed to work when ambient temperature went down to 10°C. If we recall Figure 3.4 in Chapter 3, the voltage of battery drops with temperature. When temperature was below 10°C, battery voltage, which was the total voltage of 2 batteries in series, dropped below the threshold of flash memory chip. Again, microcontroller and temperature sensor were still working properly, but it could not write any data to flash memory.

4.2.5 ADC Error Estimation

10-bit ADC in the microcontroller was used to convert the analog temperature sensor output signal to digital numbers. When we set the reference point of the ADC to be 5V, ADC test

results in Table 4.2 showed that the ADC error was less than 3%. However, if we need more precise ADC results, we can use MSP430F2013 microcontroller which has a 16-bit sigma-delta ADC, at the cost of higher power consumption.

Table 4.2: ADC test results.

Input voltage	5.00	4.06	3.86	3.30	2.27	1.91	0.79	0.16	0.00
ADC Results	1023	840	784	670	472	395	170	34	0

4.3 Validation Phase II (Batch Validation)

In validation study phase II, our main goal was to determine the accuracy of temperature measurement. Since continuous flow test was not available, we only focused on batch test (zero relative velocity between the fluid and particle).

4.3.1 Mild Temperature Tests

Before we tried to measure the accuracy of our sensor, we wanted to make sure that every component was working properly. So we did a short and mild temperature (around 70°C) measurement. Results are shown in Figure 4.5. The blue dots in Figure 4.5 are the complete temperature recorded by data acquisition device, while the pink ones are the first temperatures stored in each page of flash memory. If putting accuracy question aside, we can see the sensor is working correctly. It may be worth noting that in the very beginning the sensor is always a little hotter than room ambient temperature. We believe it was due to the touching and other activities that take place around the sensor during the packaging and preparation stage.

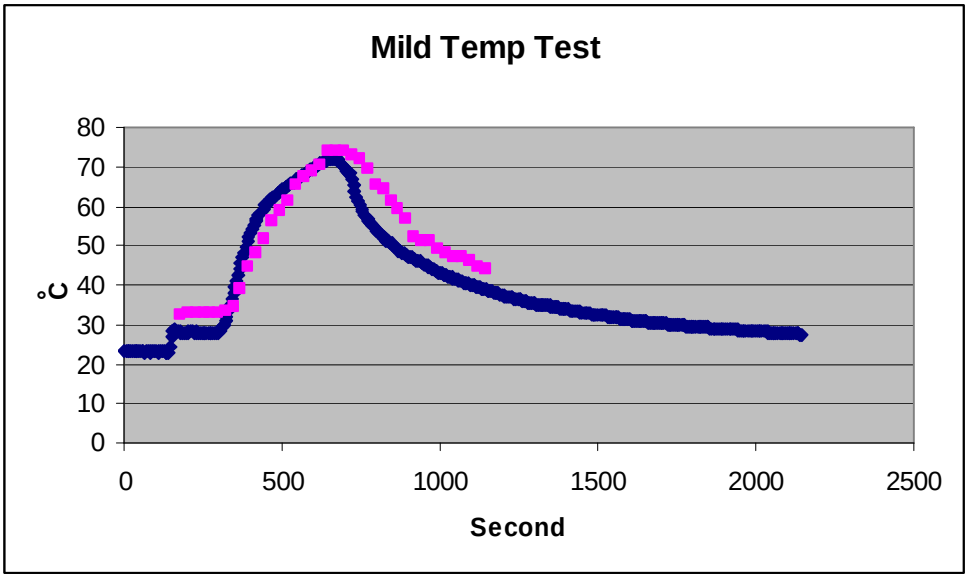

Figure 4.5: A mild temperature test (blue: temperature recorded by data acquisition device; pink: temperature points recorded in flash memory).

4.3.2 Temperature Recording Noise

Although in Figure 4.5 it showed smooth temperature transition, there were small up and down variations by looking into each page. Even though the overall plot showed the temperature rising as expected, these small variations up and down variations in temperature, as shown in Figure 4.6, were of our concern. Since ambient temperature was always higher that the temperature of sensor, we would expect a consistent rise without the small retreats.

By observing Figure 4.6, the largest variation in plot is about 1.5°C. According to data sheet, temperature sensor accuracy is +/- 1.8°C in -50°C to 70°C. So the variations are still within acceptable range. There are some techniques that could help to reduce this variation. The

pink dots in Figure 4.6 were the temperature data after taking average of every 5 samples. Result demonstrated that this method had effectively eliminated the small up and down variations in the temperature record.

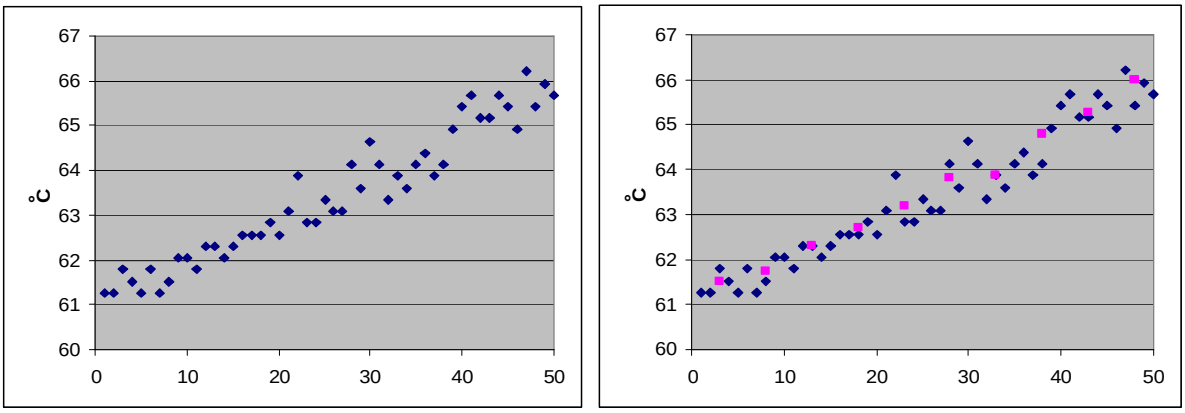

Figure 4.6: Temperature variations (left: original data; right: data after averaging).

One drawback of this method is that it decreases the sampling rate. Other techniques to suppress the variation include oversampling, median filtering, better PCB design, decent power plan, larger decoupling cap, etc.

4.3.3 High Temperature Tests

Figure 4.7 shows the results from a high temperature test. Sampling rate was 10 per second. Ideally, we would expect the blue line and pink line 100% overlap with each other. But apparently in this case, these two curves parted from each other by up to 10°C. After a few additional tests, we figured out why they failed to match. It was because, although the thermocouple was stuck in the package, it was still away from where the temperature sensor

actually was. That was why the blue curve changed sometime before the pink one does, and also why the peak of temperatures recorded in flash memory was lower than the peak of the blue curve.

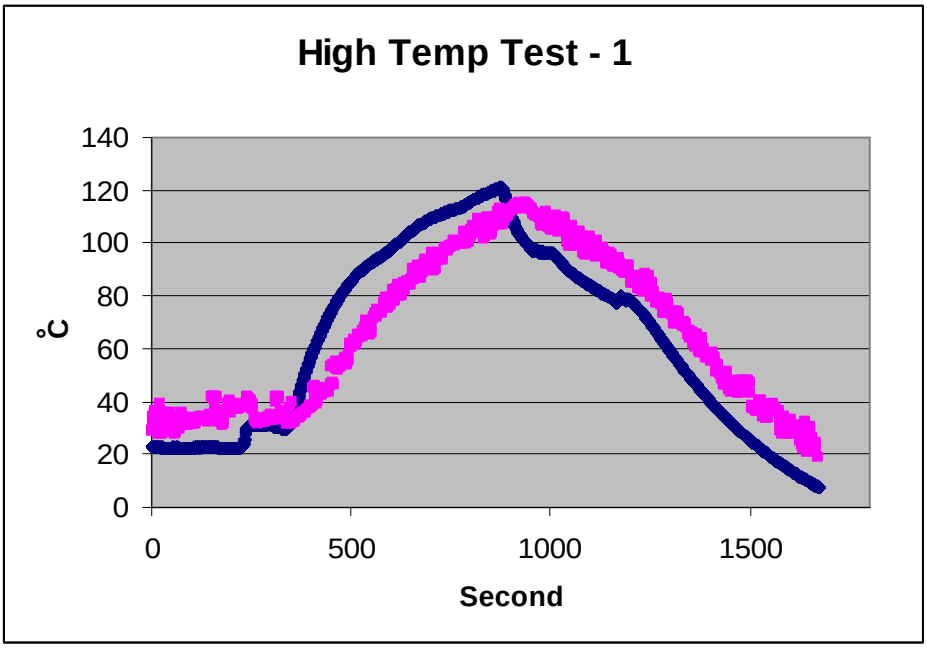

Figure 4.7: High temperature test results (blue: temperature recorded by data acquisition device; pink: temperature points recorded in flash memory).

Since the thermocouple was not fixed in the package, it had chance to move inside of the sphere. When it touched the batteries, wires, or came close to the inner surface of the sphere, abnormal reading occurred, just like what happened in Figure 4.7 when temperature was dropping. There were also variations in the temperature recording, as shown in Figure 4.8. Those variations were eliminated by median filtering. Results are shown in Figure 4.9.

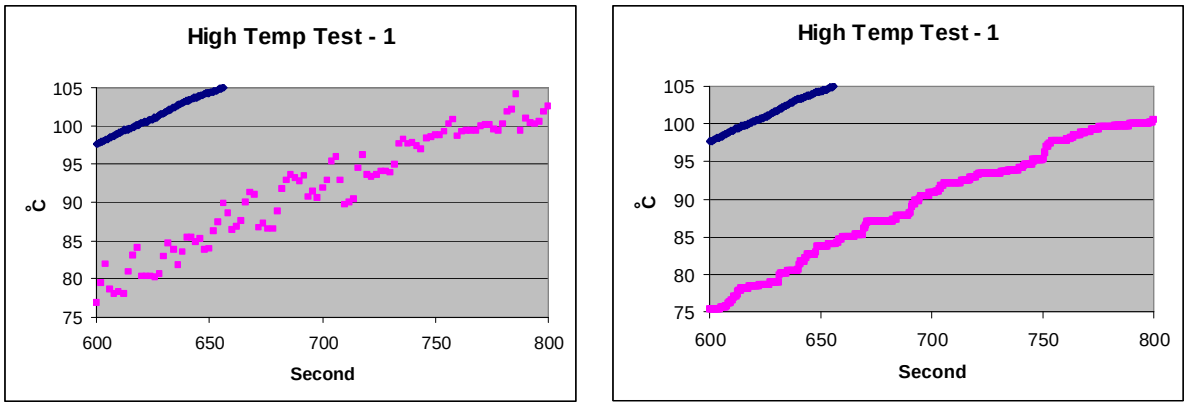

Figure 4.8: Temperature variations (left: original data; right: data after filtering).

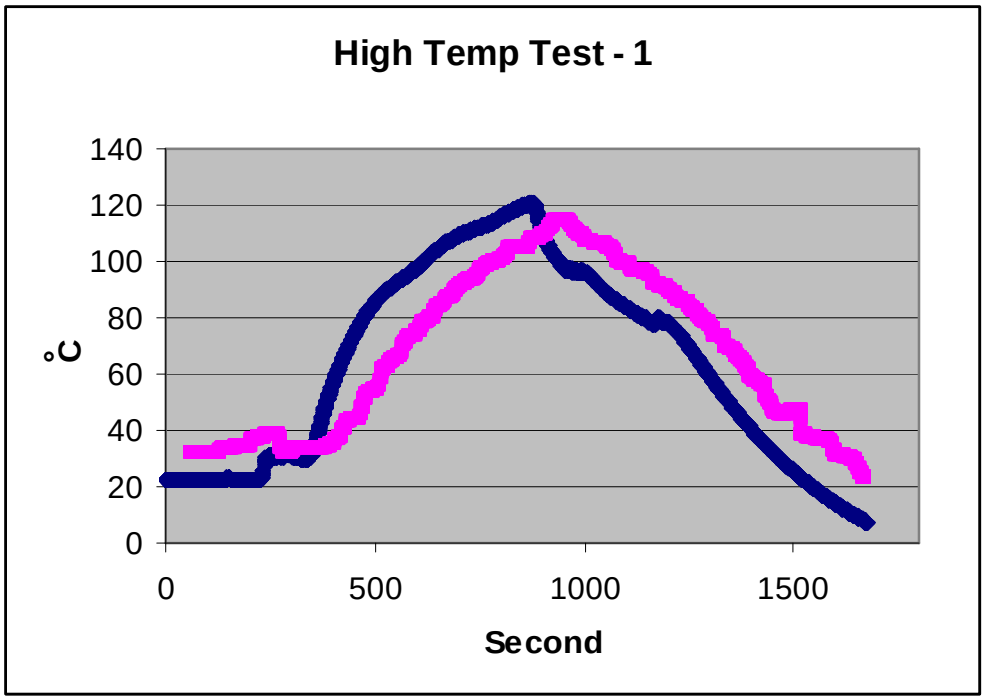

Figure 4.9: Temperature reading after filtering.

Additional high temperature tests had been done. As shown in Figure 4.10, the two curves were much closer to each other. We believed that was due to a shorter distance between the thermocouple and the temperature sensor.

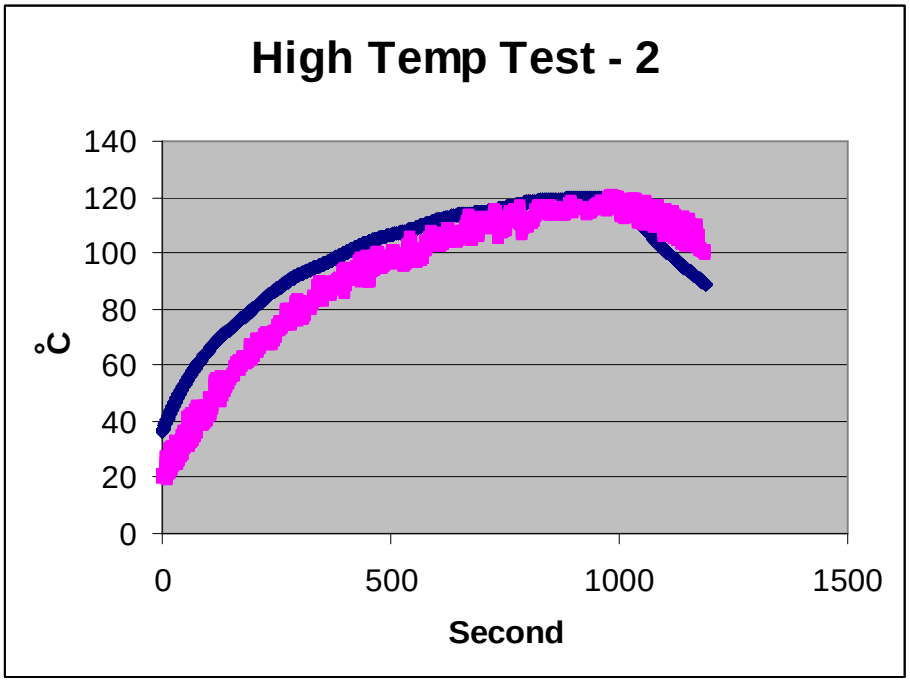

Figure 4.10: High temperature test results (blue: temperature recorded by data acquisition device; pink: temperature points recorded in flash memory).

We had also processed the data with median filtering technique. Results are shown in Figure 4.11. Since the two curves almost overlapped at their peaks, it gave us a good opportunity to estimate the accuracy of our temperature sensor. From Figure 4.12, we found out that the difference between them was less than 1°C. Taking into account that thermocouple reading should be slight higher, the actual difference was even smaller.

We still could not declare that the accuracy of our sensor was less than 1°C, due to the fact that the accuracy range of the data acquisition unit was +/- 1.25°C. However we had strong reasons to believe that we could make the accuracy within +/- 1°C, after a precise calibration with a fine temperature measurement tool.

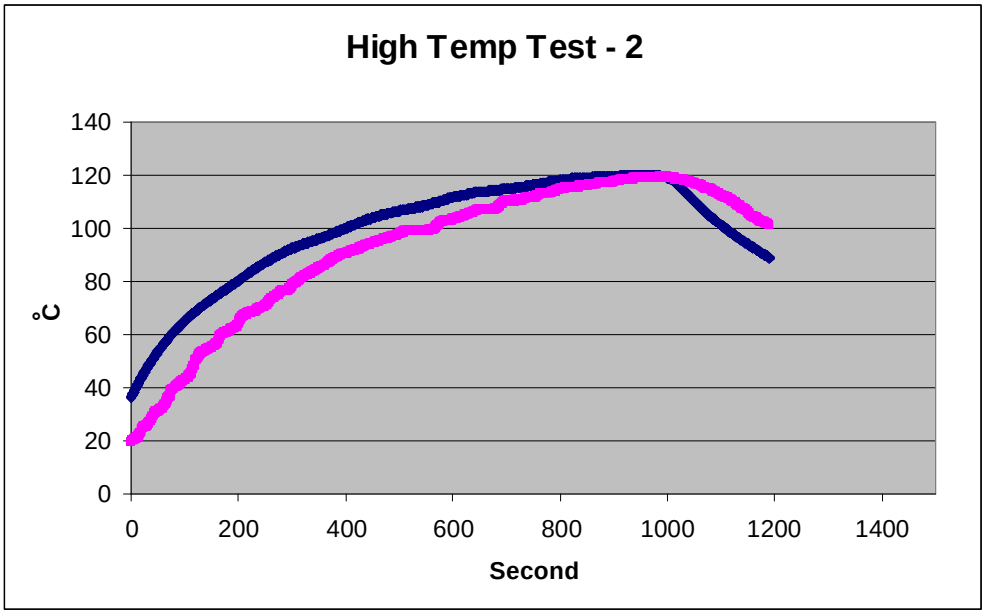

Figure 4.11: Temperature reading after filtering.

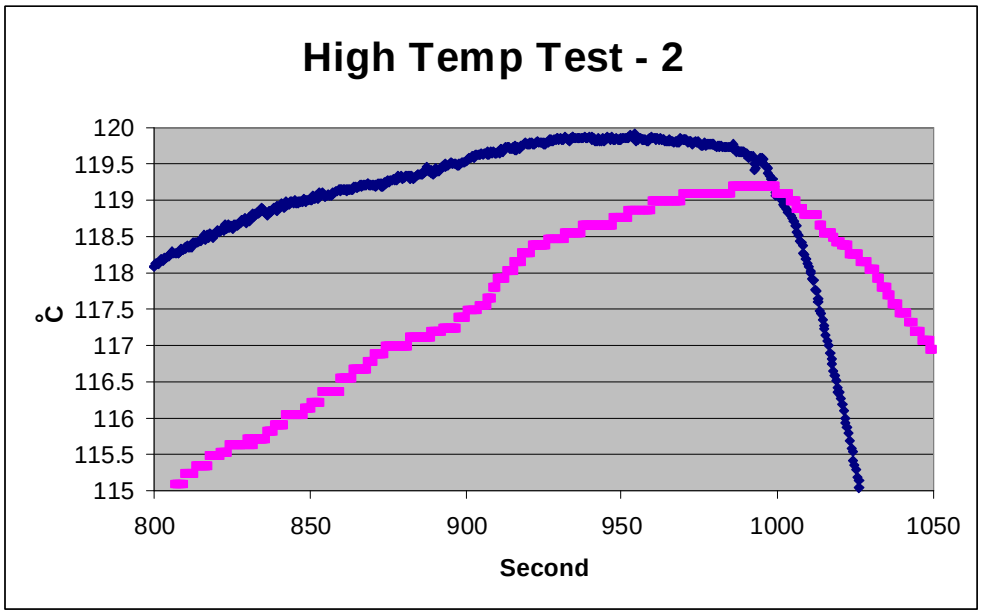

Figure 4.12: Temperature test results (zoomed in).

4.1 Discussion and Proposed Improvement

4.1.1 Temperature Variations

Low sampling rate would help reduce the variations in temperature recording. Figure 4.13 shows the results from one of our tests with sampling rate at one per second. Although there were still small variations, it was clearly much smoother than what we obtained from tests at high sampling rate. Using larger capacitor also helps, and we should try to let batteries and capacitor stay as close to the device as them could.

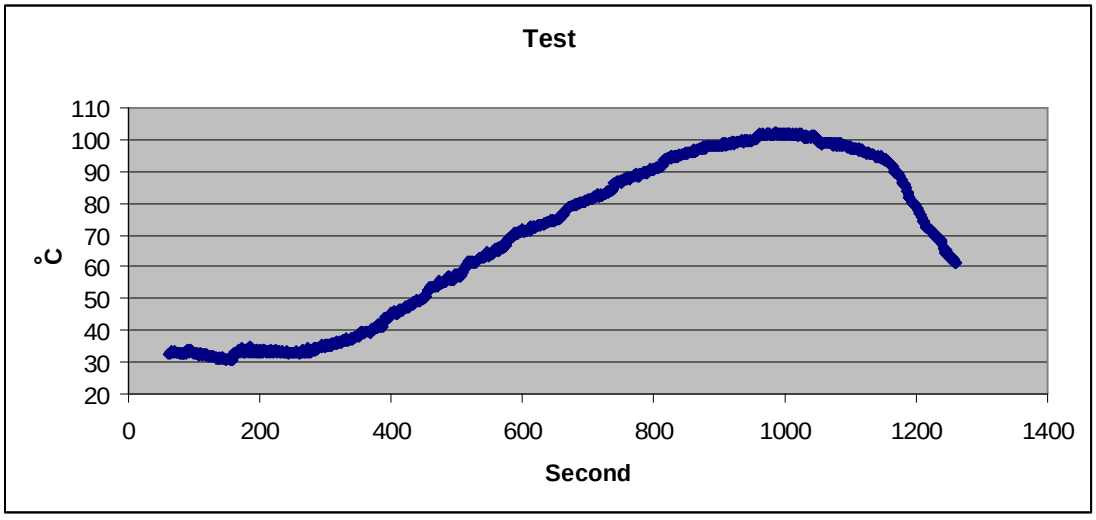

Figure 4.13: Temperature test at low sampling rate.

4.1.2 Temperature Sensor Calibration

Temperature sensor was first calibrated using the curve provided in data sheet. As our testing results indicated, it worked out pretty good. Therefore no additional calibration has been done so far. Another reason is that most fine calibrations are done in liquids. Since we did not want to put our sensor in water, we had to figure out some other ways to do it. With a

well-controlled furnace and a precise thermal sensor, we can re-calibrate our temperature sensor and improve its overall performance.

4.1.3 Other Components

There are some other components we might want to consider, as listed in Table 4.3. The reasons that they were not used in our project in the first place are also specified below. Originally we wanted to limit our sensor size to be 8mm by 8mm by 8mm. Since we had switched to a 1" sphere package later due to the density requirement, lots of them might be reconsidered for our project.

Table 4.3: Other possible components.

	Memory	Battery	Microcontroller	Sensor
Device	Atmel Flash Memory 2.5V version	BR1623A	MSP430F2013	MAX6641
Features	Lower threshold voltage requirement	120 mAh, higher nominal voltage	16-bit sigma-delta ADC	+/-1°C Accuracy
Reasons	N/A on market	Size	Power	Size (3 mm x 5 mm x 0.9 mm)
Comments	Can increase sensor working range	16mm diameter; 1.5 gram	Have to change codes	-40 to 125°C; Digital Output

CHAPTER 5

CMOS Sensor Design

While off-the-shelf sensors being developed and tested, integrated CMOS temperature sensor was also investigated. Thanks to the advanced IC processing technology, CMOS sensors are able to provide low-cost and high-performance solutions in the area of temperature sensing [30-31]. There are various kinds of CMOS temperature sensors being used in many fields in the industry as well as in household equipment [32-33]. Typical applications include: 1) the environment temperature monitor, used in automatic manufacturing factories; 2) the temperature control of consumer electronics, such as automobiles and home electronics; and 3) the power consumption control in VLSI chips, such as CPU and chip sets; and 4) the thermal compensation in single-chip systems and micro systems with built-in sensors.

Almost all the devices available in a CMOS process exhibit temperature dependent characteristics. During the last two decades, many temperature sensors have been proposed and developed, utilizing IC elements like MOS transistor, bipolar, temperature-dependent resistor, PN diode, etc [34-36]. Due to their superior temperature sensitivity and stability over MOS transistors, the bipolar temperature sensors have dominated for many years. With the advancement of its fabrication technology, more interests have been attracted to CMOS

sensors because of lower cost and better compatibility. Recently there has been a growing interest in designing a new family of CMOS sensors, called smart sensors or integrated sensors, which refers to the sensors with on-board analog to digital converters [37-40]. Because of the digital interface requirement, CMOS sensors are therefore more favorable. Compared to off-the-shelf temperature sensors, the CMOS sensors have the advantages of smaller area (less than 1 mm^2) and lower power consumption (less than 1 mW). Also it is possible to be incorporated in other techniques such as RFID. It is able to provide precise measurements with an accuracy of 1°C or less after a two point calibration, without any complicated curvature correction. The disadvantages of CMOS sensors include high development cost and poor expansibility.

In this chapter, we first review the different types of CMOS temperature sensors in section 5.1. In section 5.2, we present our CMOS sensor design with simulation results.

5.1 CMOS Sensor Overview

Numerous CMOS temperature sensors have been design for various applications [41]. In this thesis, they are categorized, by their output types, into three groups: 1) analog temperature sensors; 2) conventional digital temperature sensors; and 3) novel digital temperature sensors. Analog temperature sensor is the first member of CMOS sensor family. In this group of sensors, temperature is measured by the change of either voltage or current in one or several devices. Common analog temperature sensing techniques take advantages of either diodes, bipolar or MOS transistors [35-36]. In terms of output type, all those sensors provide

analog output signals i.e. current-output signals or voltage-output signal. In order to interface between the analog sensor and the digital environment, ADC (analog to digital converter) has been developed to output digital signals. Because of its reliable performance in most low-frequency applications, more than half of CMOS sensors are using sigma-delta A/D converters [38]. However, despite of its excellent performance, sigma-delta A/D converters have complex structures and are not area-efficient. Therefore, many digital temperature sensors have been designed with different ADC schemes. Several research groups are dealing with the design of ring-oscillator-based temperature sensors. For example, a temperature-dependent resistor can be use to control the charging/discharging current of the oscillator stages [42]. In this way, the temperature data is converted to a shift in the oscillation frequency. Another example is a time-digital-converter-based temperature sensor [39]. It is proposed for low-cost, low-power and high-accuracy on-chip integrations. One of its delay lines consists of multiple temperature compensated delay cells to reduce the thermal sensitivity. In contrast, another delay line is composed of an even number of NOT gates (or multiple equivalent delay buffers) without thermal compensation. A counter is used to count the circulation times of the input interval and generates the corresponding digital output.

5.2 CMOS Temperature Sensor Design

5.2.1 Design Overview

Based on the discussion above and our experience with off-the-shelf sensor, we came up with a CMOS temperature sensor design, as shown in Figure 5.1. It included an analog temperature sensor, a current to frequency converter, an internal clock, and a digital control

unit. The output signal of the current to frequency converter was a square-wave which carried the temperature information from the sensor. This frequency was then turned into a digital number by counting the square-wave pulses in the digital control unit, and it stored the information in the flash memory.

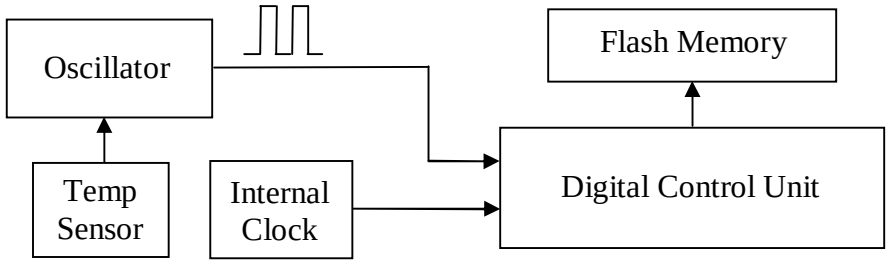

Figure 5.1: Scheme of CMOS temperature sensor design.

5.2.2 Temperature Sensor and Frequency Converter

The schematic of temperature sensor and frequency converter is shown in Figure 5.2. It was originally designed by Vladimir Szekely with the Technical University of Budapest, Hungary [43]. The first part of this circuit was a temperature with current output, and the second part was a current to frequency converter which generated square-wave carrying the temperature information. The p-channel transistor M1, M2, M3, and M4 constituted a cascade current mirror, which mirrored the current of M6 to transistor M5 and M7. Being in another current mirror, the current in M8 and M11 followed the current in M5 and M7. The main advantage of this circuit was the stable operation. The output current and the V_C and V_D voltages were

practically independent of the supply voltage. The voltages at nodes C and D could be expressed as

$$V_C = V_T(1 + \frac{X_{12}}{X_{12} - X_{67} - X_{65}}) \quad (1)$$

$$V_D = V_T(1 + \frac{X_{67}}{X_{12} - X_{67} - X_{65}}) \quad (2)$$

where Xpq was the size ratio of transistor p and transistor q.

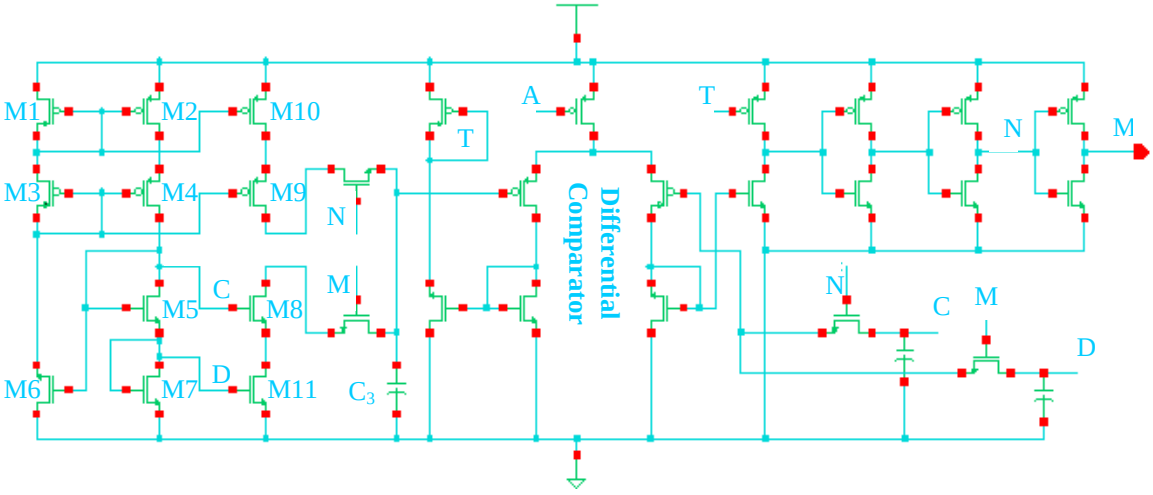

Figure 5.2: Schematic of temperature sensor and frequency converter.

The current output of the sensing circuit I_{M8} was controlled by voltage V_D, which was temperature dependent. Thus it led us to the following expression:

$$I_{M8} = b_{M11} V_T^2 (\frac{X_{67}}{X_{12} - X_{67} - X_{65}})^2 = CV_T^2 \quad (3)$$

$$\frac{\Delta I_{M8}}{I_{M8}} = \left(\frac{1}{b}\frac{db}{dT} + \frac{2}{V_T}\frac{dV_T}{dT} \right) \Delta T \quad (1)$$

where C was a constant, and V_T and β were for n-channel transistors.

The current to frequency converter was built using a simple differential comparator. The output current of the analog sensor I_{M8} and the current generated by a current mirror I_{M9} charged and discharged the capacitor C_3. The signal of the capacitor was one of the inputs to a differential comparator. The reference voltage of the comparator was switched by voltages V_C and V_D. By comparing those two signals, the differential comparator outputted a square wave. The waveforms of the comparator are shown in Figure 5.3.

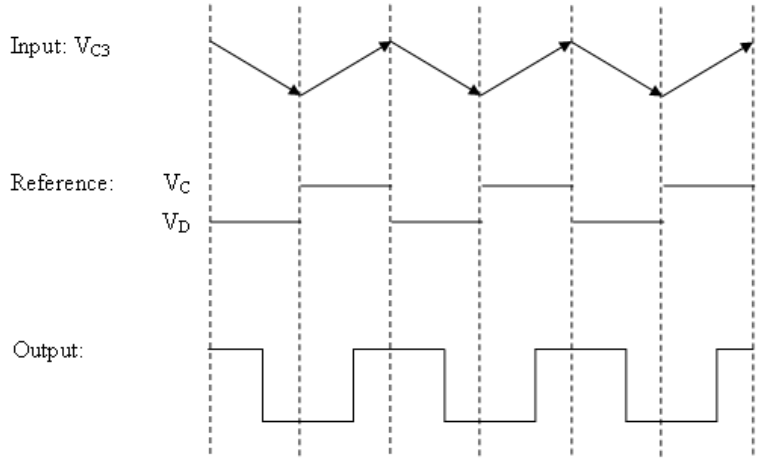

Figure 5.3: Waveforms of differential comparator.

The output of the differential comparator was sent to a series of inverters, resulted the final frequency of:

$$f = \frac{I_{M8}}{2 \cdot C_3 (V_C - V_D)} \tag{2}$$

Because the current output I_{M8}, V_C and V_D voltages were all independent of the supply voltage, the resulting frequency was also independent of the supply voltage.

5.2.3 Internal Clock

Current starved ring oscillator is a good candidate as internal clock generator in low power systems. In our project, the independence of the clock to both of the supply voltage and temperature was required to store temperature information at a stable rate in the flash memory. The schematic of a temperature compensated ring oscillator is shown in Figure 5.4. It is originally designed by Namjun Cho with the Korea Advanced Institute of Science and Technology [44].

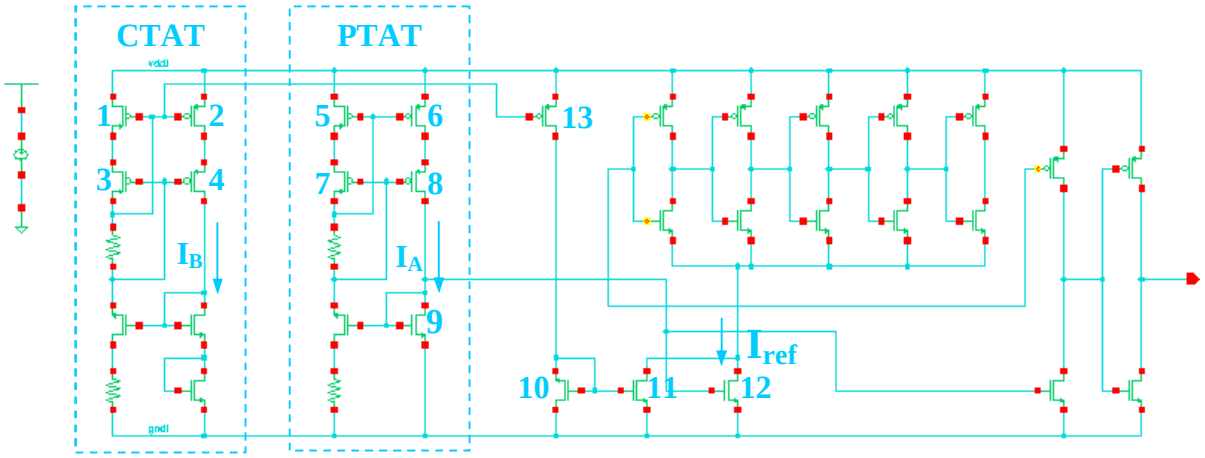

Figure 5.4: Schematic of internal clock.

A CTAT (complementary to absolute temperature) circuit was on the left side, generating a bias current I_B which was decreasing with temperature rising. Next to the CTAT is a PTAT (proportional to absolute temperature) circuit with a current I_A increasing with temperature. The current I_B was mirrored by transistor pair M2 and M13, and then mirrored by transistor pair M10 and M11. The current I_A was mirrored by transistor pair M9 and M12. By carefully matching the magnitude of these two currents, the bias current I_{ref}, which was the sum of those two, became independent of temperature and was supplied to the current starved ring oscillator. In order to suppress the sensitivity of output frequency to supply voltage changes, cascade current mirrors were used, which was constituted of transistor M1, M2, M3, and M4 in the CTAT circuit and of transistor M5, M6, M7, and M8 in the PTAT circuit. Thus the clock circuit generated an output frequency that was independent of both supply voltage and ambient temperature.

The frequency of the internal clock was set to be 2 MHz. At this frequency, the sampling rate could go as high as 1000 times per second. In case we don't need such high rate, the clock frequency can be reduced to save power.

5.2.3 Digital Control Unit Design

The digital control unit was a digital ASIC circuit, designed in Verilog and synthesized in Synopsys. Figure 5.5 shows the high level block diagram of the ASIC. It had 3 inputs, including clock, sensor frequency output, and a 3-bit "Delay_Control" signal which determined the sampling rate of our CMOS sensor.

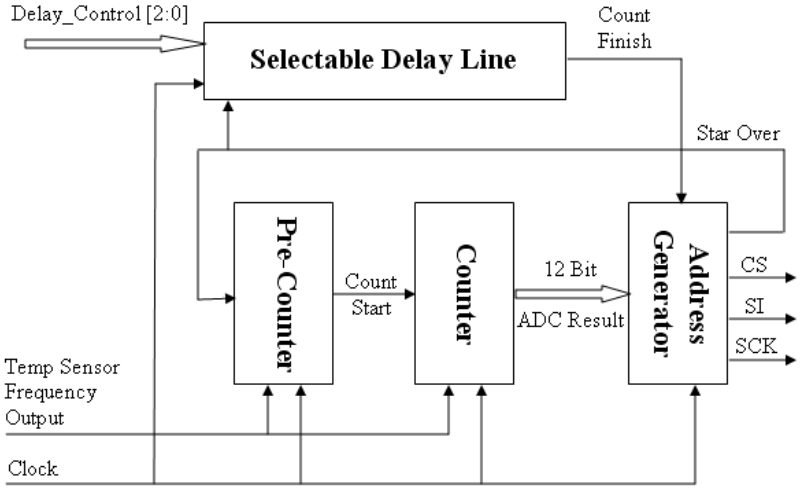

Figure 5.5: Block diagram of digital control unit.

This ASIC consisted of four main parts, pre-counter, counter, selectable delay line, and address generator. When the circuit started to work, the "pre-counter" determined when the counter should begin (it began at the next rising edge of the sensor signal). The "counter" was the block where 12-bit ADC was done. When "counter" received the "count start" signal, it began counting at every rising edge of the clock for 255 cycles of the temperature sensor's output. At the 256^{th} rising edge of the sensor signal, the ADC was finished and thus the frequency signal was converted to a 12-bit digital result.

The "selectable delay line" let user to decide the length of the delay by altering the 3-bit "Delay_Control" signal. Therefore users were able to change the sampling speed of the CMOS sensor. When "selectable delay line" ended, the "address generator" started to work.

It first generated the appropriate page and byte addresses, and then clocked the ADC results into the flash memory through three pins, CS, SI and SCK. When it finished, it sent out a "start over" signal and a new round began until the end of the memory was reached.

5.2.4 Simulation Results

A. Performance

The clock circuit generated a clock signal at 2 MHz. It was very stable over temperature variations, with sensitivity less than 0.02 %/°C. The simulated frequency output of the temperature sensor versus ambient temperature is shown in Figure 5.6. The frequency varied from 0.98 MHz to 0.21 MHz at the temperature range of 0°C to 150°C. The slope was about -0.97 %/°C.

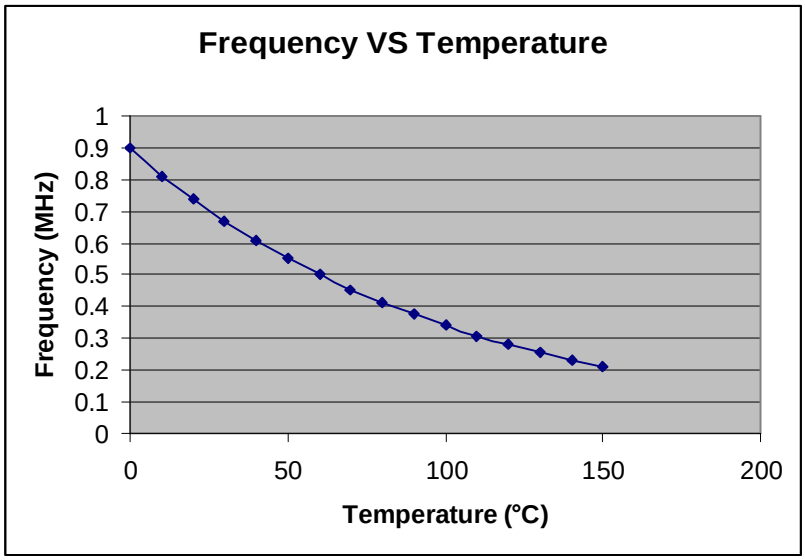

Figure 5.6: Frequency output versus ambient temperature.

Figure 5.7 shows the waveforms of the ASIC circuit over first a few sample cycles, and Figure 5.8 focuses on the output waveforms of the address generator. When the ADC was done and “count finish” signal was on, the address generator started to work by sending out opcode 82H, followed by 11-bit page address and 9-bit byte address. Then the 12-bit ADC result had been clocked out. After that it set “start over” signal high and new A/D conversion began. The sampling speed could change from 1 to 1000 samples per second, selectable by end users. The ADC accuracy was less than 0.1°C.

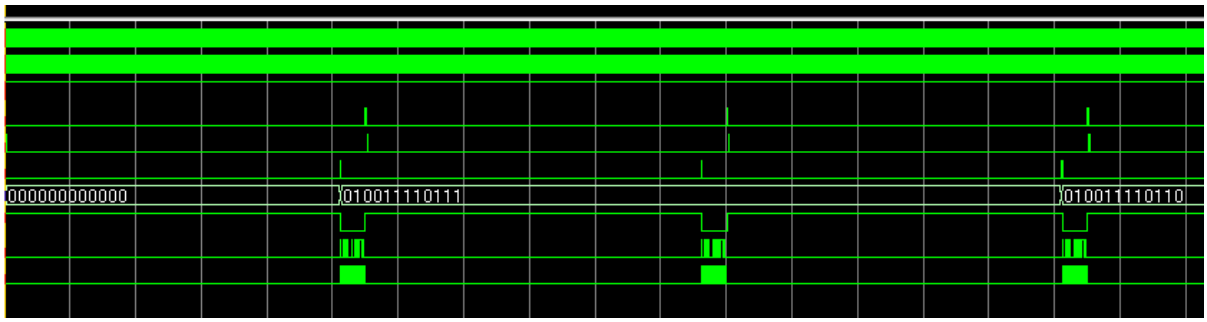

Figure 5.7: ASIC circuit waveforms.

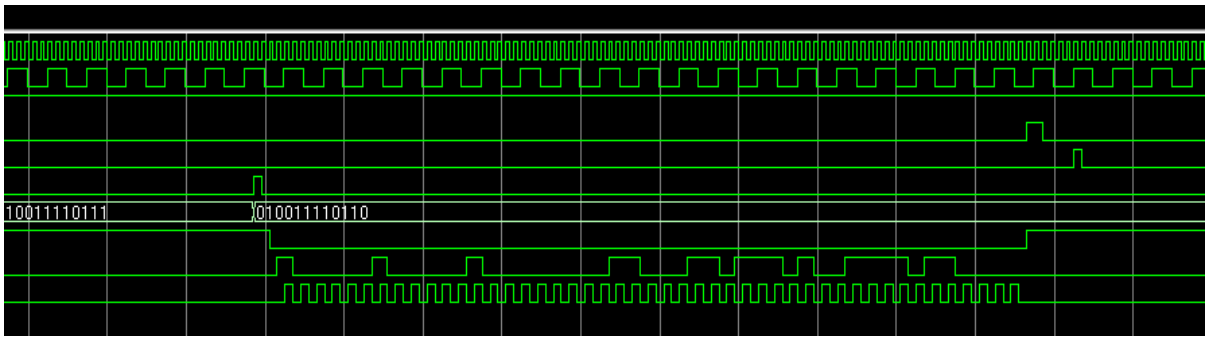

Figure 5.8: Detailed ASIC circuit output waveforms.

B. Layout and Size

The layout of both of the clock and the temperature sensor was completed in IBM 7RFML 180nm process. The layout is shown in Figure 5.9, with a total area of 0.0085 mm^2.

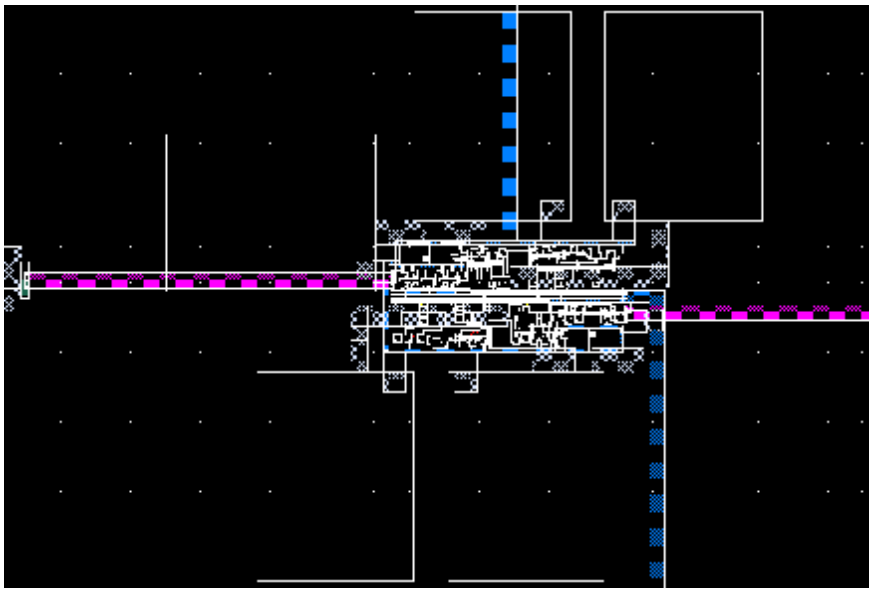

Figure 5.9: Layout of the clock and the temperature sensor.

The ASIC was synthesized in Synopsys, and then placed and routed in Encounter with iit018 standard cell library. The final layout is shown in Figure 5.10, with a total area of 0.045 mm^2.

C. Power

Power consumption is a very important parameter in our project. The power of the sensing circuit was 0.015 - 0.019 mW, and the power of the clock circuit was 0.47 - 0.51 mW. The power consumption of clock circuit was a little high due to the temperature compensation.

Without that, the clock was able to run at extremely low current. The evaluation of the power consumption of the ASIC was little more complicated. It involved the determination of the switching activity associated with the nets in the design, so it had to be done after routing, with a test fixture of its typical activities. Simulation in design complier showed that the whole power consumption was 0.284 mW, with 0.193 mW on clock.

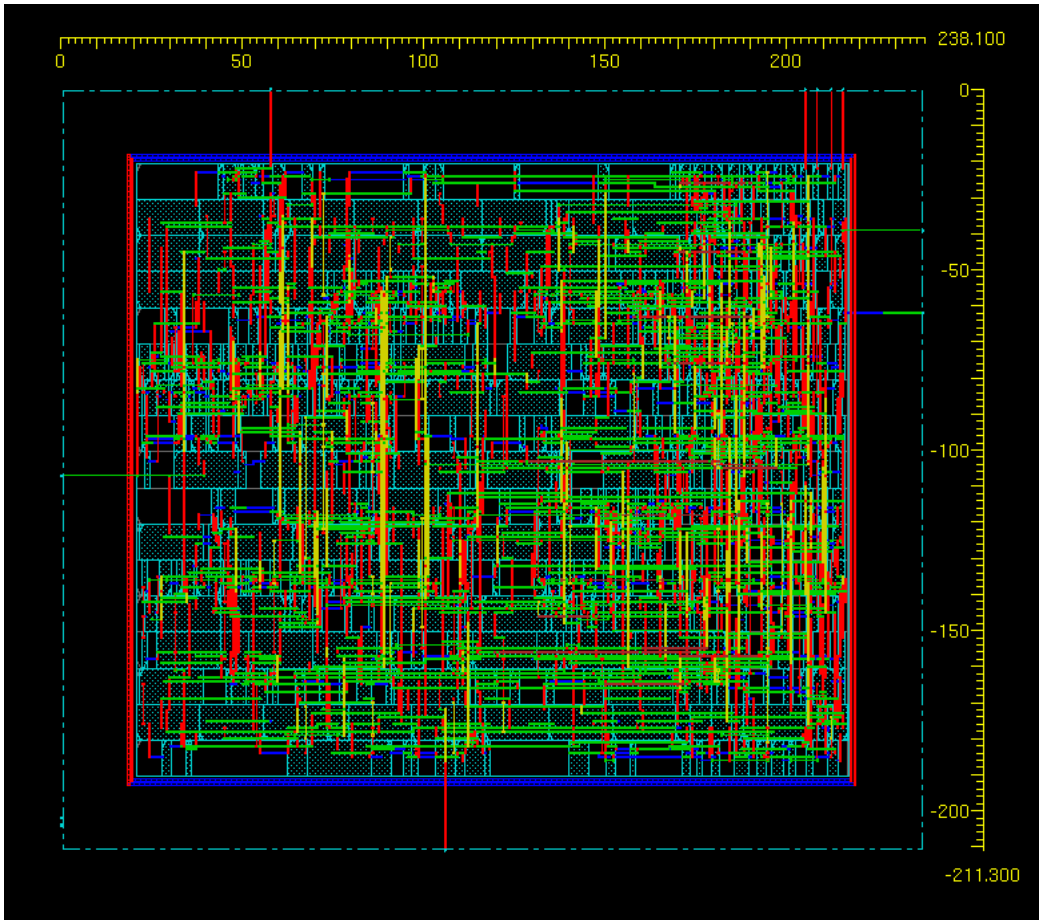

Figure 5.10: Layout of the digital control unit.

D. Summary

Table 5.1 contains the summary of our CMOS sensor, over a temperature range from 0°C to 150°C. The CMOS sensor had a total area of 0.054 mm^2, an averaged power consumption of 0.8 mW, and an accuracy of less than 0.2°C.

Table 5.1: Technical summary of CMOS sensor.

	Size (mm^2)	Power (mW)	Output (Hz)	Sensitivity
Temp Sensor	0.0085	0.015 - 0.019	0.21M – 0.89M	$\Delta f/(f*\Delta T) = 0.97$ %
Clock		0.47 - 0.51	2.0M	$\Delta f/(f*\Delta T) < 0.02$ %
Digital Unit	0.045	0.284	1 - 1000	ADC Accuracy < 0.1°C
Total	0.054	0.76 – 0.91	-	Accuracy < 0.2°C

CHAPTER 6

Conclusion and Future Work

5.1 Conclusion

Food safety is rapidly becoming one of the most critically important issues in food industry. With the increasing consumer demand for convenient, high quality, and healthy foods, aseptic processing was proposed as a potential option to meet these demands. In order to validate such a system and also make the process relatively inexpensive, researchers have to find out the "critical particle" in the processing system and determine its time-temperature history.

To address this problem, we started to develop low-power and high-performance sensors that could be applied to monitor the internal temperature of particulates, as they went through the heating, holding, and cooling sections of an aseptic processing system. Battery-powered off-the-shelf sensor had been successfully designed and tested. It was packaged in 1" plastic sphere, and the density was neutrally buoyant with water. It was able to work in the temperature range of 10°C to 150°C, with a potential accuracy of less than 1°C. The battery could last more than 20 hours.

While the off-the-shelf sensors being designed and tested, integrated CMOS temperature sensor had also been investigated. Compared to off-the-shelf temperature sensors, the CMOS sensors have the advantages of smaller area and lower power consumption. The CMOS sensor design and simulation results have been presented in details in Chapter 5. It had a total area of 0.054 mm^2, an averaged power consumption of 0.8 mW, and an accuracy of less than 0.2°C.

The significance of this study lies in the development of a validated tool and technique that can be used to facilitate validating aseptic processing of multiphase foods and thereby provide the health-conscious consumer with a high quality food product. The results of our project can be useful to food processors for conducting validation studies as part of the process filing procedure for multiphase food products. Our sensors and testing methodology can be used to demonstrate to the FDA or USDA that the simulated particle will have conservative heating and flow characteristics which will ensure the adequacy of the process and the safety of the food product.

The sensor will be useful not only for validating aseptic processing of low-acid foods containing particulates, but also in improving the quality of high-acid foods undergoing a hot-fill process and for low-acid refrigerated foods. It can also be used in applications where temperature “indicators” are used instead of actual time-temperature data. Thus, the demands of the consumer for convenient and high quality foods can be met. An additional benefit of the success of this technology would be the development of new food products that were

hitherto unavailable due to their potentially low quality (due to the inherent over-processing in a typical retort canning process).

5.2 Future Work

Apart from the work that has been done with respect to the development of temperature sensors for food processing, the future work will involve additional testing and validation, device miniaturization and optimization, and design of CMOS sensor with on-board memory and RF telemetry.

5.2.1 Off-the-shelf Sensor

Modification is needed to help reduce the noise in temperature recording. With a well-controlled furnace and a precise thermal sensor, the off-the-shelf sensor can be re-calibrated and its overall performance will be improved. More batch tests need to be done, and continuous flow tests also need to be started to ensure that the sensor system would conservatively determine the temperature within the particle at any intermediate processing condition, over the widest possible range of parameters.

Off-the-shelf sensor needs to be optimized and miniaturized, while satisfying the density and function requirements. Under current size, we can consider some new components, such as digital temperature sensor, to improve the performance of the sensor. With the help of new technology and product, thin-film battery for instant, we can further shrink the size of our sensor to less than ½" in diameter.

5.2.2 CMOS Sensor and RFID

CMOS temperature sensor has been design in this thesis. However it is just a prototype without on-board memory and RF telemetry, which are desired for our project. Further research has to be done to incorporate these elements in the CMOS sensor. Other techniques including on chip antenna, battery-less operation and position tracking system may also be investigated for this project.

As being discussed before, accurate determination of the time-temperature history at critical point in a system will greatly simplify the validation process for any aseptic food processing. The use of RFID (Radio Frequency Identification) combined with our temperature sensor is a promising technique to solve this problem [45-46].

RFID is a general term that is used to describe a system that transmits the identity of an object using radio waves [47]. Communication takes place between a reader and a transponder often called a tag. Tags can either be active (powered by battery) or passive (powered by the reader field), and come in various forms including smart cards, tags, labels, watches and even embedded in mobile phones. The communication frequencies used depends to a large extent on the application, and range from 125 KHz to 2.45 GHz. RFID has many applications including many familiar ones such as vehicle security, commuter tags and security badges for access control into buildings.

An RFID system is used not only to transmit signals, or to indicate its location. When the RFID is combined with other sensory systems, its application area can be wildly extended to environmental monitoring such as temperature, humidity and pressure sensing, as well as wireless data transmission [48-49]. All these features therefore make it very attractive in the area of food industry and retail supply chain management.

In our project, we plan to take the advantage of RFID technology to capture and transmit internal temperatures of food particles while they are travelling through food processing system. The easiest way to accomplish this is to incorporate a passive RFID tag in our off-the-shelf sensor package, so that it could "tell" the detector outside of the tube when it passes certain locations. An off-the-shelf transponder could be a better alternative, since it will not only report the location but also transmit the instantaneous temperature readings to the detector.

For our CMOS sensor design, we have also proposed several methods to incorporate RFID in our design. Figure 6.1 presents a simple design with a RC rectifier. When receiving RF signals from outside RF transmitter, it converts the RF power to a digital "1" and this will be save in the flash memory together with the temperature records. So if we search the memory after tests we can find out when it comes cross the RF transmitter. Another plan is to have an on-board RF transmitter, as shown in Figure 6.2, so that it enables on-line wireless temperature data transfer. A basic design of the transmitter includes just a mixer and a power

amplifier. The clock signal that has been generated in the digital control unit can be used as carrier wave.

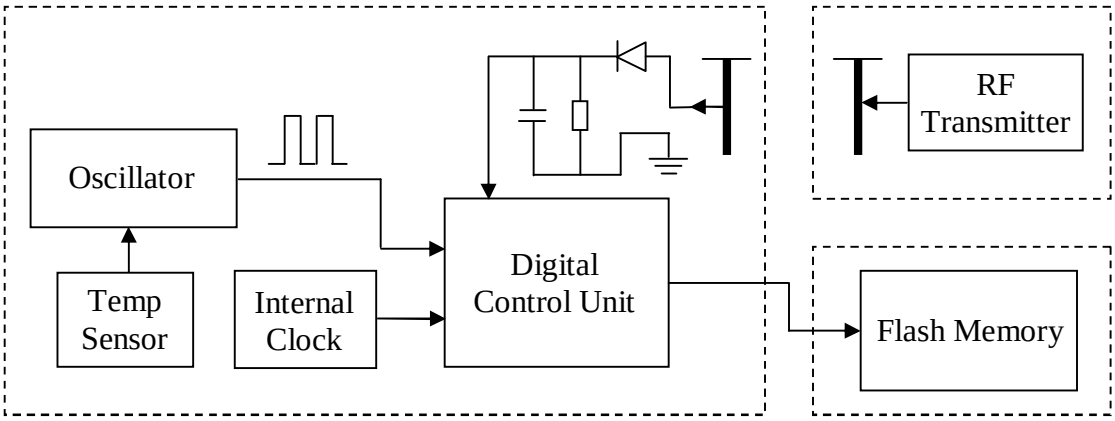

Figure 6.1: CMOS sensor with simple RF receiver.

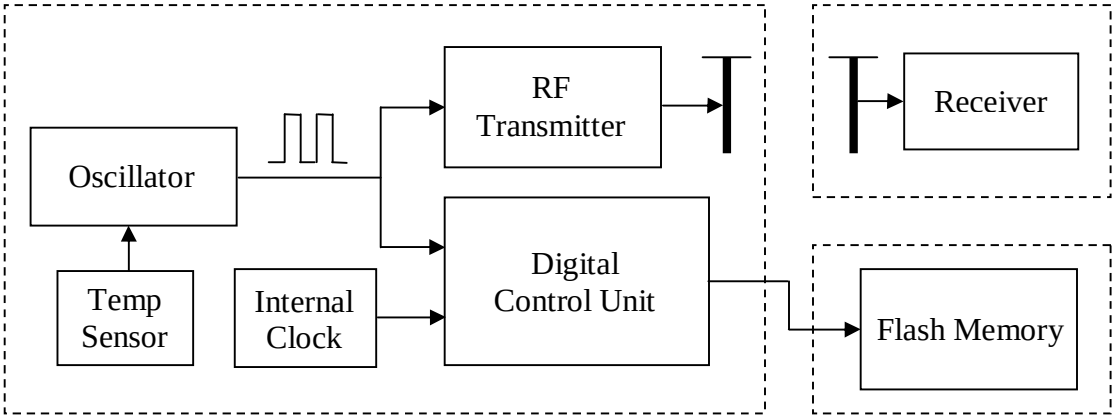

Figure 6.2: CMOS sensor with on-chip RF transmitter.

With the help of RFID technology, we would be enabled to the process lethality, cook value and perform an optimization to maximize product quality. If we can develop a validated RFID system that can be used to transmit information regarding the internal temperatures of particles, it will be very helpful in process filing, improving quality of food products, and enhancing the safety of a continuous thermal process. It will also be very valuable in ascertaining the degree of product deterioration during transportation and storage, thereby enabling the processor & retailer to modify the transportation and storage conditions to improve quality and enhance shelf-life of food products.

Bibliography

[1] Guiavarc'h, Y., Dintwa, E., Van, L., Ann., Z.F., and Hendrickx, M. Validation and use of an enzymic time temperature integrator to monitor thermal impacts inside a solid/liquid model food. *Biotechnology Progress*. Vol. 18(5): 1087-1094, 2002.

[2] Morris-Lee, J. CAPPS develops validation technologies for multiphase aseptic processing. *Aseptic processing and packaging*. Vol. 1(2): 5, 14-21, 2004.

[3] Dignan, D.M., Berry, M.R., Pflug, I.J., and Gardine, T.D. Safety considerations in establishing aseptic processes for low acid foods containing particulates. *Food Technol*. 43(3): 118, 1989.

[4] CAPPS and NCFST. Case study for condensed cream of potato soup from the aseptic processing of multiphase foods workshops, Nov. 14-15, 1995 and March 12-13, 1996.

[5] Larkin, J.W. Continuous multiphase aseptic processing of foods. *Food Technology*. Vol. 51(10): 43-44, 1997.

[6] Chandarana, D.I. Acceptance procedures for aseptically processed particulate foods. In *Advances in aseptic processing technologies*. Edited by R.K. Singh and P.E. Nelson. Elsevier Applied Sciences, London. pp. 261-278, 1992.

[7] Kantt, C.A., Schmidt, S.J., Sizer, C.E., Palaniappan, S., and Litchfield, J.B. Temperature mapping of particles during aseptic processing with magnetic resonance imaging. *Journal of Food Science*. Vol. 63(2): 305-311, 1998.

[8] Heppell, N.J. Comparison of the residence time distributions of water and milk in an experimental UHT sterilizer. *Journal of Food Process Engineering*. Vol. 4: 71-84, 1985.

[9] Cacase, D., Palmieri, L., Pirone, G., and Dipollina, G. Biological validation of mathematical modeling of the thermal processing of particulate foods: The influence of heat transfer coefficient determination. *Journal of Food Engineering*. Vol. 23: 51-68, 1994.

[10] Tobback, P., Hendrickx, M.E., Weng, Z., Maesmans, G.J., and DeCordt, S.V. The use of immobilized enzymes as time temperature indicator system in thermal processing. In

Advances in Food Engineering. Editors: R.P. Singh and M.A. Wirakartakusumah. CRC Press Inc., Boca Raton, FL. pp. 561-574, 1992.

[11] Sastry, S.K. Liquid to particle heat transfer coefficient in aseptic processing. In *Advances in Aseptic Processing Technologies*. Editors: R.K. Singh and P.E. Nelson. Elsevier Applied Science, London. pp. 63-72, 1992.

[12] Zitoun, K.B. and Sastry, S.K. Convective heat transfer coefficient for cubic particles in continuous tube flow using the moving thermocouple method. *Journal of Food Process Engineering*. Vol. 17: 229-241, 1994.

[13] Zitoun, K.B. and Sastry, S. Determination of convective heat transfer between fluid and cubic particles in continuous tube flow using noninvasive experimental techniques. *Journal of Food Process Engineering*. Vol. 17: 209-228, 1994.

[14] Stoforos, N.G. and Merson, R.L. Measurement of heat transfer coefficients in rotating liquid/particulate systems. *Biotechnology Progress*. Vol. 7: 267-271, 1991.

[15] Hendrickx, M., Weng, Z., Maesmans, G., and Tobback, P. Validation of a time temperature integrator for thermal processing of foods under pasteurization conditions. *International Journal of Food Science and Technology*. Vol. 27: 21-31, 1992.

[16] Guiavarc'h, Y., Deli, V., Van, L.A., and Hendrickx, M. Development of an enzymic time temperature integrator for sterilization process based on *Bacillus licheniformis* a-amylase at reduced water content. *Journal of Food Science*. Vol. 67(1): 285-291, 2002.

[17] Mwangi, J.M., Rizvi, S.S.H., and Datta, A. Heat transfer to a particle in shear flow: application in aseptic processing. *Journal of Food Engineering*. Vol. 19: 55-74, 1993.

[18] Ghiron, K. M.,and Lithchfield, J. B. Magnetic thermometry in the aseptic processing of foods containing particulates. *Journal of Applied Physics*. Vol. 81(8): 4321, 1997.

[19] Beller, L. S. Ultrasonic tomography for in-process measurements of temperature in a multi-phase medium. U.S. Patent No. 5,181,778. U.S. Patent and Trademark Office, U.S. Department of Commerce, Alexandria, VA, 1993.

[20] Reiffel, L. X-ray imaged implanted thermometers. U.S. Patent No. 6,250,800. U.S. Patent and Trademark Office, U.S. Department of Commerce, Alexandria, VA, 2001.

[21] Kantt, C.A., Webb, A.G., and Litchfield, J.B. Temperature measurement of foods using chemical shift magnetic resonance imaging as compared with T1-weighted temperature mapping. *Journal of Food Science*. Vol. 62(5): 1011-1016, 1997.

[22] Kantt, C.A., Schmidt, S.J., Sizer, C.E., Palaniappan, S., and Litchfield, J.B. Temperature mapping of particles during aseptic processing with magnetic resonance imaging. *Journal of Food Science*. Vol. 63(2): 305-311, 1998.

[23] Simunovic, J. Particle flow monitoring in multiphase aseptic systems. Ph.D. Thesis, North Carolina State University, Raleigh, NC, 1998.

[24] Palazoglu, T.K., Simunovic, J., Sandeep, K.P., and Swartzel, K.R. Methods, systems and devices for evaluation of thermal treatment. European Patent No. WO2004067786. European Patent Office, 2004.

[25] Nam, S.K., Yin, S. High-temperature sensing using whispering gallery mode resonance in bent optical fibers. *IEEE Photonics Technology Letter*, vol. 17, no. 11, 2005.

[26] http://www.picotech.com/applications/temperature.html

[27] http://www.labfacility.co.uk/news/53

[28] http://focus.ti.com/mcu/mcuprodoverview.tsp?sectionId=95&tabId=140&familyId=342

[29] http://industrial.panasonic.com/jvcr13pz.cgi?E+BA+3+AAA4002+BR1225A+7+WW

[30] G. C. M. Meijer. Thermal sensors based on transistors. *Sensors and Actuators*, vol. 10, pp. 103-125, 1986.

[31] Szekely et al. CMOS temperature sensors and built-in test circuitry for thermal testing of ICs. *Sensors and Actuators, A: Physical*, vol. 71, pp. 10-18, 1998.

[32] Krummenacher, P., Oguey, H. Smart temperature sensor in CMOS technology. *Sensors and Actuators*, vols. A21L.423, pp. 636-638, 1990.

[33] Yu, H., Najafi, K. Low-power interface circuits for bio-implantable Microsystems. In *IEEE Int, Solid-State Circuits Conf. Dig. Tech. Papers*, pp. 194 – 487, Feb. 2003.

[34] MontanC, E., Bota, S.A. A compact temperature sensor of a 1.0 pm CMOS technology using lateral PNP transistors. *THERMINIC'96 Workshop Proceedings*, pp.45-4.8, Budapest, Hungary, Sep. 1996.

[35] SzCkely, V., Mirta, C., Kohiri, Z. New temperature sensors for DfTT' applications. *THERMINIC'96 Workshop Proceedings*, pp.49-55, Budapest, Hungary, Sep. 1996.

[36] Qutnot, G.M., Paris, N. A temperature and voltage measurement cell for VLSI circuits. *Euro-Asic '91,* pp.334-338, 1991.

[37] Bota, S.A., Rosales, M., Segura, J. L. J. Smart temperature sensor for thermal testing of cell-based ICs. In *Proceedings of the Design, Automation and Test in Europe Conference and Exhibition,* pp. 1530-1591, 2005.

[38] Bakker, A., Huijsing, J.H. Micropower CMOS smart temperature sensor. *ESSCIRC'95,* Lille, France, Proceedings pp.238-241, Sep. 1995.

[39] Chen, P., Chen, C-C., Tsai, C-C., and Lu, W-F. A time-to-digital-converter-based CMOS smart temperature sensor. *IEEE J. Solid-State Circuits* 40 1642–8, 2005.

[40] Wang, G. and Meijer, G.C.M. The temperature characteristics of bipolar transistors fabricated in CMOS technology. *Sensors Actuators,* vol. 16, pp.23-28, 2000.

[41] Bakker, A., and Huijsing, J.H. CMOS smart temperature sensor an overview. *Proc. IEEE Sensors* 2 1423–7, 2000.

[42] Bakker, A., and Huijsing, J.H. A low-cost high-accuracy CMOS smart temperature sensor *Proc. ESSCIRC* 25 302–5, 1999.

[43] SzCkely, V., Mirta, C., Kohiri, Z. CMOS sensors for on-line thermal monitoring of VLSI circuits. *IEEE Tran. On VLSI Systems*, vol. 5, no. 3, Sep., 1997.

[44] Cho, N., Song, S-J., and Yoo, H-J. An 8-uW, 0.3-mm2 RF-powered transponder with temperature sensor for wireless environmental monitoring. *IEEE International Symposium on Circuits and Systems (ISCAS),* Kobe, Japan, May 25, 2005.

[45] Lewis, S. A basic introduction to RFID technology and its use in the supply chain, *Laran* RFID*, White paper*, 2004.

[46] Glidden, R., Bockorick, C., et al. Design of ultra-low-cost UHF RFID tags for supply chain applications. *IEEE Communications Magazine*, August 2004.

[47] Finkenzeller, K. RFID Handbook. *John Wiley & Sons*, pp. 53-104, 1999.

[48] Huang, Q., and Oberle, M. A 0.5-mW passive telemetry IC for biomedical applications. *IEEE Journal of Solid-state Circuits*, vol. 33, pp. 937-946, 1998.

[49] Wang, T.H. and Ker, M.D. On-chip ESD protection design by using polysilicon diodes in CMOS technology for smart-card applications. In *Proc. EOS/ESD Symp.*, pp. 266–275, 2000.